

# Best Available Copy

(12) INTERNATIONAL APPLICATION PUBLISHED UNDER THE PATENT COOPERATION TREATY (PCT)

(19) World Intellectual Property Organization  
International Bureau



(43) International Publication Date  
24 October 2002 (24.10.2002)

PCT

(10) International Publication Number  
WO 02/084213 A1

(51) International Patent Classification: G01B 11/00,  
G03F 9/00, G01N 21/86

Street, 30900 Zichron Yaakov (IL). FRIEDMANN,  
Michael; 23/2 Hazait Street, 36760 Nesher (IL). FAEYR-  
MAN, Michael; 28/12 Menachim Begin Street, 26100  
Kiryat Motzkin (IL).

(21) International Application Number: PCT/US02/11026

(22) International Filing Date: 9 April 2002 (09.04.2002)

(74) Agent: HSUE, James, S.; Skjerven Morrill LLP, Three  
Embarcadero Center, 28th Floor, San Francisco, CA 94111  
(US).

(25) Filing Language: English

(26) Publication Language: English

(81) Designated State (national): JP.

(30) Priority Data:  
09/833,084 10 April 2001 (10.04.2001) US

(84) Designated States (regional): European patent (AT, BE,  
CH, CY, DE, DK, ES, FI, FR, GB, GR, IE, IT, LU, MC,  
NL, PT, SE, TR).

(71) Applicant: KLA-TENCOR CORPORATION [US/US];  
160 Rio Robles, San José, CA 95134-1809 (US).

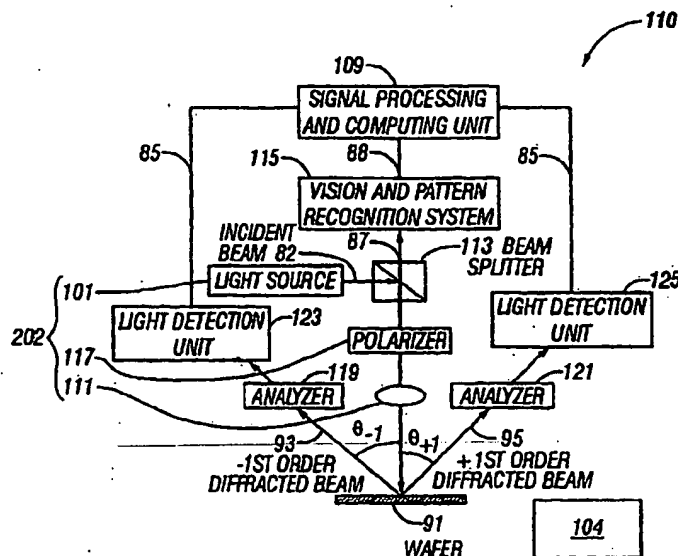
Published:

— with international search report  
— before the expiration of the time limit for amending the  
claims and to be republished in the event of receipt of  
amendments

(72) Inventors: ABDULHALIM, Ibrahim; P.O. Box 942,  
17907 Kfar Manda (IL). ADEL, Mike; 14 Yigal Alon

[Continued on next page]

(54) Title: PERIODIC PATTERNS AND TECHNIQUE TO CONTROL MISALIGNMENT



(57) Abstract: A method and system to measure misalignment error between two overlying or interlaced periodic structures (13, 15) are proposed. The overlying or interlaced periodic structures are illuminated by incident radiation from a light source (101), and the diffracted radiation of the incident radiation by the overlying or interlaced periodic structures are detected by a detector (123, 125) to provide an output signal. The misalignment between the overlying or interlaced periodic structures may then be determined from the output signal.

WO 02/084213 A1

WO 02/084213 A1



*For two-letter codes and other abbreviations, refer to the "Guidance Notes on Codes and Abbreviations" appearing at the beginning of each regular issue of the PCT Gazette.*

## PERIODIC PATTERNS AND TECHNIQUE TO CONTROL MISALIGNMENT

5

### BACKGROUND OF THE INVENTION

10

The invention relates in general to metrology systems for measuring periodic structures such as overlay targets, and, in particular, to a metrology system employing diffracted light for detecting misalignment of such structures.

Overlay error measurement requires specially designed marks to be strategically placed at various locations, normally in the scribe line area between dies, on the wafers for each process. The alignment of the two overlay targets from two consecutive processes is measured for a number of locations on the wafer, and the overlay error map across the wafer is analyzed to provide feedback for the alignment control of lithography steppers.

A key process control parameter in the manufacturing of integrated circuits is the measurement of overlay target alignment between successive layers on a semiconductor wafer. If the two overlay targets are misaligned relative to each other, then the electronic devices fabricated will malfunction, and the semiconductor wafer will need to be reworked or discarded.

Measurement of overlay misregistration between layers is being performed today with optical microscopy in different variations: brightfield, darkfield, confocal, and interference microscopy, as described in Levinson, "Lithography Process Control," chapter 5, SPIE Press Vol. TT28, 1999. Overlay targets may comprise fine structures on top of the wafer or etched into the surface of the wafer. For example, one overlay target may be formed by etching into the wafer, while another adjacent overlay target may be a resist layer at a higher elevation over the wafer. The target being used for this purpose is called box-in-box where the outer box, usually 10 to 30  $\mu\text{m}$ , represents the position of the bottom layer, while the inner box is smaller and represents the location of the upper layer. An optical microscopic image is grabbed for this target and analyzed with image processing techniques. The relative location

of the two boxes represents what is called the overlay misregistration, or the overlay. The accuracy of the optical microscope is limited by the accuracy of the line profiles in the target, by aberrations in the illumination and imaging optics and by the image sampling in the camera. Such methods are complex and they require full imaging optics. Vibration isolation is also required.

These techniques suffer from a number of drawbacks. First, the grabbed target image is highly sensitive to the optical quality of the system, which is never ideal. The optical quality of the system may produce errors in the calculation of the overlay misregistration. Second, optical imaging has a fundamental limit on resolution, which affects the accuracy of the measurement. Third, an optical microscope is a relatively bulky system. It is difficult to integrate an optical microscope into another system, such as the end of the track of a lithographic stepper system. It is desirable to develop an improved system to overcome these drawbacks.

#### SUMMARY OF THE INVENTION

A target for determining misalignment between two layers of a device has two periodic structures of lines and spaces on the two different layers of a device. The two periodic structures overlies or are interlaced with each other. The layers or periodic structures may be at the same or different heights. In one embodiment, either the first periodic structure or the second periodic structure has at least two sets of interlaced grating lines having different periods, line widths or duty cycles. The invention also relates to a method of making overlying or interlaced targets.

An advantage of the target is the use of the same diffraction system and the same target to measure critical dimension and overlay misregistration. Another advantage of the measurement of misregistration of the target is that it is free from optical asymmetries usually associated with imaging.

The invention also relates to a method of detecting misalignment between two layers of a device. The overlying or interlaced periodic structures are illuminated by incident radiation. The diffracted radiation from the overlying or interlaced periodic structures is used to provide an output signal. In one embodiment, a signal is derived from the output signal. The misalignment between the structures is determined from

the output signal or the derived signal. In one embodiment, the output signal or the derived signal is compared with a reference signal. A database that correlates the misalignment with data related to diffracted radiation can be constructed.

An advantage of this method is the use of only one incident radiation beam.

5 Another advantage of this method is the high sensitivity of zero-order and first-order diffracted light to the overlay misregistration between the layers. In particular, properties which exhibited high sensitivity are intensity, phase and polarization properties of zero-order diffraction; differential intensity between the positive and negative first-order diffraction; differential phase between the positive and negative

10 first-order diffraction; and differential polarization between the positive and negative first-order diffraction. These properties also yielded linear graphs when plotted against the overlay misalignment. This method can be used to determine misalignment on the order of nanometers.

In one embodiment, a neutral polarization angle, defined as an incident

15 polarization angle where the differential intensity is equal to zero for all overlay misregistrations, is determined. The slope of differential intensity as a function of incident polarization angle is highly linear when plotted against the overlay misregistration. This linear behavior reduces the number of parameters that need to be determined and decreases the polarization scanning needed. Thus, the method of

20 detecting misalignment is faster when using the slope measurement technique.

The invention also relates to an apparatus for detecting misalignment of overlying or interlaced periodic structures. The apparatus comprises a source, at least one analyzer, at least one detector, and a signal processor to determine misalignment of overlying or interlaced periodic structures.

25 **BRIEF DESCRIPTION OF THE DRAWINGS**

Figs. 1a-1h are cross-sectional views illustrating basic process steps in semiconductor processing.

Fig. 2a is a cross-sectional view of two overlying periodic structures. Figs. 2b and 2c are top views of the two overlying periodic structures of Fig. 2a.

Fig. 3 is a top view of two overlying periodic structures illustrating an embodiment of the invention.

Figs. 4a and 4b are cross-sectional views of overlying or interlaced periodic structures illustrating other embodiments of the invention.

5        Fig. 5a and 5b are cross-sectional views of two interlaced periodic structures illustrating interlaced gratings in an embodiment of the invention.

Fig. 6 is a cross-sectional view of two interlaced periodic structures illustrating interlaced gratings in another embodiment of the invention.

10       Figs. 7a and 7b are schematic views illustrating negative and positive overlay shift, respectively.

Fig. 8 is a schematic view illustrating the diffraction of light from a grating structure.

15       Fig. 9a is a schematic block diagram of an optical system that measures zero-order diffraction from overlying or interlaced periodic structures. Fig. 9b is a schematic block diagram of an integrated system of the optical system of Fig. 9a and a deposition instrument.

20       Figs 10a and 11a are schematic block diagrams of an optical system that measures first-order diffraction from a normal incident beam on overlying or interlaced periodic structures. Figs. 10b and 11b are schematic block diagrams of integrated systems of the optical systems of Fig. 10a and 11a, respectively, and a deposition instrument.

Figs. 12a and 12b are graphical plots of derived signals from zero-order diffraction of incident radiation on overlying structures.

25       Figs. 13-14 and 16-17 are graphical plots of derived signals from first-order diffraction of incident radiation on overlying structures. Fig. 15 is a graphical plot illustrating the mean square error.

Figs. 18-19 and 21-22 are graphical plots of derived signals from zero-order diffraction of incident radiation on interlaced gratings. Figs. 20 and 23 are graphical plots illustrating the mean square error.

Fig. 24 is a graphical plot illustrating the determination of misalignment from a slope near a neutral polarization angle.

For simplicity of description, identical components are labeled by the same numerals in this application.

### **DETAILED DESCRIPTION OF THE EMBODIMENTS**

Fig. 2a is a cross-sectional view of a target 11 comprising two periodic structures 13, 15 on two layers 31, 33 of a device 17. The second periodic structure 15 is overlying or interlaced with the first periodic structure 13. The layers and the periodic structures may be at the same or different heights. The device 17 can be any device of which the alignment between two layers, particularly layers having small features on structures, needs to be determined. These devices are typically semiconductor devices; thin films for magnetic heads for data storage devices such as tape recorders; and flat panel displays.

As shown in Figs. 1a-1h, a device 17 is generally formed in a basic series of steps for each layer. First, as shown in Fig. 1a, a layer 2 is formed on a semiconductor substrate 1. The layer 2 may be formed by oxidization, diffusion, implantation, evaporation, or deposition. Second, as shown in Fig. 1b, resist 3 is deposited on the layer 2. Third, as shown in Fig. 1c, the resist 3 is selectively exposed to a form of radiation 5. This selective exposure is accomplished with an exposure tool and mask 4, or data tape in electron or ion beam lithography (not shown). Fourth, as shown in Fig. 1d, the resist 3 is developed. The resist 3 protects the regions 6 of the layer 2 that it covers. Fifth, as shown in Fig. 1e, the exposed regions 7 of the layer 2 are etched away. Sixth, as shown in Fig. 1f, the resist 3 is removed. Alternatively, in another embodiment, another material 8 can be deposited in the spaces 7, as shown in Fig. 1e, of the etched layer 2, as shown in Fig. 1g, and the resist 3 is removed after the deposition, as shown in Fig. 1h. This basic series of steps is repeated for each layer until the desired device is formed.

A first layer 31 and a second layer 33 can be any layer in the device. Unpatterned semiconductor, metal or dielectric layers may be deposited or grown on top of, underneath, or between the first layer 31 and the second layer 33.

The pattern for the first periodic structure 13 is in the same mask as the pattern for a first layer 31 of the device, and the pattern for the second periodic structure 15 is in the same mask as the pattern for a second layer 33 of the device. In one embodiment, the first periodic structure 13 or the second periodic structure 15 is the etched spaces 7 of the first layer 31 or the second layer 33, respectively, as shown in Fig. 1f. In another embodiment, the first periodic structure 13 or the second periodic structure 15 is the lines 2 of the first layer 31 or the second layer 33, respectively, as shown in Fig. 1f. In another embodiment, the first periodic structure 13 or the second periodic structure 15 is another material 8 deposited in the spaces 7 of the first layer 31 or the second layer 33, respectively, as shown in Fig. 1h. In yet another embodiment, the second layer 33 is resist, and the second periodic structure 15 is resist 3 gratings, as shown in Fig. 1d.

The first periodic structure 13 has the same alignment as the first layer 31, since the same mask was used for the pattern for the first periodic structure 13 and for the pattern for the first layer 31. Similarly, the second periodic structure 15 has the same alignment as the second layer 33. Thus, any overlay misregistration error in the alignment between the first layer 31 and the second layer 33 will be reflected in the alignment between the first periodic structure 13 and the second periodic structure 15.

Fig. 2b and 2c are top views of target 11. In one embodiment, as illustrated in Fig. 2a, the first periodic structure 13 has a first selected width CD1, and the second periodic structure 15 has a second selected width CD2. The second selected width CD2 is less than the first selected width CD1. The pitch, also called the period or the unit cell, of a periodic structure is the distance after which the pattern is repeated. The distance between the left edge of the first periodic structure 13 and the left edge of the second periodic structure 15 is  $d_1$ , and the distance between the right edge of the first periodic structure 13 and the right edge of the second periodic structure 15 is  $d_2$ . In a preferred embodiment, when layers 31, 33 are properly aligned relative to each other, the second periodic structure 15 is centered over the first periodic structure 13. In



other words, when the second periodic structure 15 is perfectly centered over the first periodic structure 13, the misregistration is zero, and  $d_1=d_2$ . In this embodiment, the misregistration is indicated by  $d_2-d_1$ . To obtain misregistration in both the X and Y directions of the XY coordinate system, another target 12 comprising two periodic structures 14, 16 similar to target 11 is placed substantially perpendicular to target 11, as shown in Fig. 2c.

The target 11 is particularly desirable for use in photolithography, where the first layer 31 is exposed to radiation for patterning purposes of a semiconductor wafer and the second layer 33 is resist. In one embodiment, the first layer 31 is etched silicon, and the second layer 33 is resist.

Figs. 4a and 4b show alternative embodiments. In one embodiment, Fig. 4a illustrates a first periodic structure 13 of oxide having a trapezoidal shape on a first layer 31 of silicon substrate and a second periodic structure 15 of resist with a second layer 33 of resist. The first layer 31 of silicon is etched, and shallow trench isolation ("STI") oxide is deposited in the spaces of the etched silicon. The lines of STI oxide form the first periodic structure 13. An oxide layer 34 and a uniform polysilicon layer 35 are deposited between the first layer 31 of silicon and the second layer 33 of resist. The configuration in Fig. 4a shows a line on space configuration, where the second periodic structure 15 is placed aligned with the spaces between the first periodic structure 13. The invention also encompasses embodiments such as the line on line configuration, where the lines in the second periodic structure 15 are placed on top of and aligned with the lines in the first periodic structure 13, as shown by the dotted lines in Fig. 4a.

In another embodiment, Figure 4b illustrates a first periodic structure 13 of tungsten etched in a first layer 31 of oxide and a second periodic structure 15 of resist with a second layer 33 of resist. The first layer 31 and the second layer 33 are separated by an aluminum blanket 37.

The invention relates to a method of making a target 11. A first periodic structure 13 is placed over a first layer 31 of a device 17. A second periodic structure 15 is placed over a second layer 33 of the device 17. The second periodic structure 15 is overlying or interlaced with the first periodic structure 13.

In one embodiment, another target 12 is placed substantially perpendicular to target 11, as shown in Fig. 2c. A third periodic structure 14 is placed over the first layer 31, and a fourth periodic structure 14 is placed over the second layer 33. The third periodic structure 14 is substantially perpendicular to the first periodic structure 13, and the fourth periodic structure 16 is substantially perpendicular to the second periodic structure 15.

An advantage of the target 11 is that the measurement of misregistration of the target is free from optical asymmetries usually associated with imaging. Another advantage of this measurement is that it does not require scanning over the target as it is done with other techniques, such as in Bareket, U.S. Patent 6,023,338. Another advantage of the target 11 is the elimination of a separate diffraction system and a different target to measure the critical dimension ("CD") of a periodic structure. The critical dimension, or a selected width of a periodic structure, is one of many target parameters needed to calculate misregistration. Using the same diffraction system and the same target to measure both the overlay misregistration and the CD is more efficient. The sensitivity associated with the CD and that with the misregistration is distinguished by using an embodiment of a target as shown in Fig. 3. The second periodic structure 15 extends further to an area, the CD region 21, where the first periodic structure 13 does not extend. The first selected width CD1 is measured before placing the second periodic structure 15 on the device 17. After forming the target, the second selected width CD2 alone can be measured in the CD region 21. In a separate measurement, the misregistration is determined in an overlay region 19 where both the first 13 and second 15 periodic structures lie.

Fig. 5a and 5b are cross-sectional views of an embodiment of a target having interlaced gratings. The first periodic structure 13 or the second periodic structure 15 has at least two interlaced grating lines having different periods, line widths or duty cycles. The first periodic structure 13 is patterned with the same mask as that for the first layer 31, and the second periodic structure 15 is patterned with the same mask as that for the second layer 33. Thus, the first periodic structure 13 has the same alignment as the first layer 31, and the second periodic structure 15 has the same alignment as the second layer 33. Any misregistration between the first layer 31 and

the second layer 33 is reflected in the misregistration between the first periodic structure 13 and the second periodic structure 15.

In the embodiment shown in Figs. 5a and 5b, the first periodic structure 13 has two interlaced grating lines 51, 53. The first interlaced grating lines 51 have a line-width  $L_1$ , and the second interlaced grating lines 53 have a line-width  $L_2$ . The second periodic structure 15, as shown in Fig. 5b, has a line-width  $L_3$  and is centered between the first interlaced grating lines 51 and the second interlaced grating lines 53. The distance between the right edge of the first interlaced grating 51 and the adjacent left edge of the second interlaced grating 53 is represented by  $b$ , and the distance between the right edge of the second periodic structure 15 and the adjacent left edge of the second interlaced grating 53 is represented by  $c$ . The misregistration between the first layer 31 and the second layer 33 is equal to the misregistration  $\epsilon$  between the first periodic structure 13 and the second periodic structure 15. The misregistration  $\epsilon$  is:

(1)

$$\epsilon = \frac{b}{2} - \frac{L_2}{2} - c$$

Where  $c=0$ , the resulting periodic structure has the most asymmetric unit cell composed of a line with width of  $L_1+L_3$  and a line with width  $L_2$ . Where  $c=b-L_3$ , the resulting periodic structure has the most symmetric unit cell composed of a line with width  $L_1+L_3$  and a line with width  $L_2$ . For example, if the two layers are made of the same material and  $L_1=L_3=L_2/2$ , then the lines are identical where  $c=0$ , while one line is twice as wide as the other line where  $c=b-L_3$ .

Fig. 6 shows an alternative embodiment of a target having interlaced gratings. The first periodic structure 13 is etched silicon, and the second periodic target 15 is resist. The first layer 31 of silicon substrate and the second layer 33 of resist are separated by an oxide layer 39.

The invention also relates to a method of making a target 11. A first periodic structure 13 is placed over a first layer 31 of a device 17. A second periodic structure 15 is placed over a second layer 33 of the device 17. The second periodic structure 15 is overlying or interlaced with the first periodic structure 13. Either the first periodic

structure 13 or the second periodic structure 15 has at least two interlaced grating lines having different periods, line widths or duty cycles.

An advantage of interlaced gratings is the ability to determine the sign of the shift of the misregistration from the symmetry of the interlaced gratings. Figs. 7a and 7b are schematic drawings illustrating negative and positive overlay shift, respectively, in the X direction of the XY coordinate system. Center line 61 is the center of a grating 63. When the grating 63 is aligned perfectly, the center line 61 is aligned with the Y axis of the XY coordinate system. As shown in Fig. 7a, a negative overlay shift is indicated by the center line 61 being in the negative X direction. As shown in Fig. 7b, a positive overlay shift is indicated by the center line 61 being in the positive X direction. The negative overlay shift is indicated by a negative number for the misregistration, and the positive overlay shift is indicated by a positive number for the misregistration. The misregistration can be determined using the method discussed below. In the case of the interlaced gratings, a negative overlay shift results in a more symmetrical unit cell, as where  $c=b-L_3$ , discussed above. A positive overlay shift results in a more asymmetrical unit cell, as where  $c=0$ , discussed above.

The invention relates to a method to determine misalignment using diffracted light. Fig. 8 is a schematic view showing the diffraction of light from a grating structure 71. In one embodiment, incident radiation 73 having an oblique angle of incidence  $\theta$  illuminates the grating structure 71. The grating structure 71 diffracts radiation 75, 77, 79. Zero-order diffraction 75 is at the same oblique angle  $\theta$  to the substrate as the incident radiation 73. Negative first-order diffraction 77 and positive first-order diffraction 79 are also diffracted by the grating structure 71.

Optical systems for determining misalignment of overlying or interlaced periodic structures are illustrated in Figs. 9a, 10a, and 11a. Fig. 9a shows an optical system 100 using incident radiation beam 81 with an oblique angle of incidence and detecting zero-order diffracted radiation 83. A source 102 provides polarized incident radiation beam 81 to illuminate periodic structures on a wafer 91. The incident radiation beam may be substantially monochromatic or polychromatic. The source 102 comprises a light source 101 and optionally a collimating/ focusing/ polarizing optical module 103. The structures diffract zero-order diffracted radiation 83. A

collimating/ focusing/ analyzing optical module 105 collects the zero-order diffracted radiation 83, and a light detection unit 107 detects the zero-order diffracted radiation 83 collected by the analyzer in module 105 to provide an output signal 85. A signal processor 109 determines any misalignment between the structures from the output  
5 signal 85. The output signal 85 is used directly to determine misalignment from the intensity of the zero-order diffracted radiation 83. In a preferred embodiment, the misalignment is determined by comparing the intensity with a reference signal, such as a reference signal from a calibration wafer or a database, compiled as explained below. In one embodiment, the signal processor 109 calculates a derived signal from  
10 the output signal 85 and determines misalignment from the derived signal. The derived signal can include polarization or phase information. In this embodiment, the misalignment is determined by comparing the derived signal with a reference signal.

In one embodiment, optical system 100 provides ellipsometric parameter values, which are used to derive polarization and phase information. In this  
15 embodiment, the source 102 includes a light source 101 and a polarizer in module 103. Additionally, a device 104 causes relative rotational motion between the polarizer in module 103 and the analyzer in module 105. Device 104 is well known in the art and is not described for this reason. The polarization of the reflected light is measured by the analyzer in module 105, and the signal processor 109 calculates the  
20 ellipsometric parameter values,  $\tan(\Psi)$  and  $\cos(\Delta)$ , from the polarization of the reflected light. The signal processor 109 uses the ellipsometric parameter values to derive polarization and phase information. The phase is  $\Delta$ . The polarization angle  $\alpha$  is related to  $\tan(\Psi)$  through the following equation:

(2)

25

$$\tan \alpha = \frac{1}{\tan \Psi}$$

The signal processor 109 determines misalignment from the polarization or phase information, as discussed above.

The imaging and focusing of the optical system 100 in one embodiment is verified using the vision and pattern recognition system 115. The light source 101

provides a beam for imaging and focusing 87. The beam for imaging and focusing 87 is reflected by beam splitter 113 and focused by lens 111 to the wafer 91. The beam 87 then is reflected back through the lens 111 and beam splitter 113 to the vision and pattern recognition system 115. The vision and pattern recognition system 115 then  
5 sends a recognition signal 88 for keeping the wafer in focus for measurement to the signal processor 109.

Fig. 10a illustrates an optical system 110 using normal incident radiation beam 82 and detecting first-order diffracted radiation 93, 95. A source 202 provides polarized incident radiation beam 82 to illuminate periodic structures on a wafer 91.  
10 In this embodiment, the source 202 comprises a light source 101, a polarizer 117 and lens 111. The structures diffract positive first-order diffracted radiation 95 and negative first-order diffracted radiation 93. Analyzers 121, 119 collect positive first-order diffracted radiation 95 and negative first-order diffracted radiation 93, respectively. Light detection units 125, 123 detect the positive first-order diffracted  
15 radiation 95 and the negative first-order diffracted radiation 93, respectively, collected by analyzers 121, 119, respectively, to provide output signals 85. A signal processor 109 determines any misalignment between the structures from the output signals 85, preferably by comparing the output signals 85 to a reference signal. In one embodiment, the signal processor 109 calculates a derived signal from the output  
20 signals 85. The derived signal is a differential signal between the positive first-order diffracted radiation 95 and the negative first-order diffracted radiation 93. The differential signal can indicate a differential intensity, a differential polarization angle, or a differential phase.

Optical system 110 determines differential intensity, differential polarization  
25 angles, or differential phase. To determine differential phase, optical system 110 in one embodiment uses an ellipsometric arrangement comprising a light source 101, a polarizer 117, an analyzer 119 or 121, a light detector 123 or 125, and a device 104 that causes relative rotational motion between the polarizer 117 and the analyzer 119 or 121. Device 104 is well known in the art and is not described for this reason. This  
30 arrangement provides ellipsometric parameters for positive first-order diffracted radiation 95 and ellipsometric parameters for negative first-order diffracted radiation 93, which are used to derive phase for positive first-order diffracted radiation 95 and

phase for negative first-order diffracted radiation 93, respectively. As discussed above, one of the ellipsometric parameters is  $\cos(\Delta)$ , and the phase is  $\Delta$ . Differential phase is calculated by subtracting the phase for the negative first-order diffracted radiation 93 from the phase for the positive first-order diffracted radiation 95.

5 To determine differential polarization angles, in one embodiment, the polarizer 117 is fixed for the incident radiation beam 82, and the analyzers 121, 119 are rotated, or vice versa. The polarization angle for the negative first-order diffracted radiation 93 is determined from the change in intensity as either the polarizer 117 or analyzer 119 rotates. The polarization angle for the positive first-order diffracted  
10 radiation 95 is determined from the change in intensity as either the polarizer 117 or analyzer 121 rotates. A differential polarization angle is calculated by subtracting the polarization angle for the negative first-order diffracted radiation 93 from the polarization angle for the positive first-order diffracted radiation 95.

To determine differential intensity, in one embodiment, the analyzers 119, 121  
15 are positioned without relative rotation at the polarization angle of the first-order diffracted radiation 93, 95. Preferably, at the polarization angle where the intensity of the diffracted radiation is a maximum, the intensity of the positive first-order diffracted radiation 95 and the intensity of the negative first-order diffracted intensity 93 is detected by the detectors 125, 123. Differential intensity is calculated by  
20 subtracting the intensity for the negative first-order diffracted radiation 93 from the intensity for the positive first-order diffracted radiation 95.

In another embodiment, the differential intensity is measured as a function of the incident polarization angle. In this embodiment, the polarizer 117 is rotated, and the analyzers 119, 121 are fixed. As the polarizer 117 rotates, the incident  
25 polarization angle changes. The intensity of the positive first-order diffracted radiation 95 and the intensity of the negative first-order diffracted radiation 93 is determined for different incident polarization angles. Differential intensity is calculated by subtracting the intensity for the negative first-order diffracted radiation 93 from the intensity for the positive first-order diffracted radiation 95.

30 The imaging and focusing of the optical system 110 in one embodiment is verified using the vision and pattern recognition system 115. After incident radiation

beam 82 illuminates the wafer 91, a light beam for imaging and focusing 87 is reflected through the lens 111, polarizer 117, and beam splitter 113 to the vision and pattern recognition system 115. The vision and pattern recognition system 115 then sends a recognition signal 88 for keeping the wafer in focus for measurement to the  
5 signal processor 109.

Fig. 11a illustrates an optical system 120 where first-order diffracted radiation beams 93, 95 are allowed to interfere. The light source 101, device 104, polarizer 117, lens 111, and analyzers 119, 121 operate the same way in optical system 120 as they do in optical system 110. Device 104 is well known in the art and is not  
10 described for this reason. Once the negative first-order diffracted radiation 93 and positive first-order diffracted radiation 95 are passed through the analyzers 119, 112, respectively, a first device causes the positive first-order diffracted radiation 95 and the negative first-order diffracted radiation 93 to interfere. In this embodiment, the first device comprises a multi-aperture shutter 131 and a flat beam splitter 135. The  
15 multi-aperture shutter 131 allows both the negative first-order diffracted radiation 93 and the positive first-order diffracted beam 95 to pass through it. The flat beam splitter 135 combines the negative first-order diffracted radiation 93 and the positive first-order diffracted radiation 95. In this embodiment, the mirrors 127, 133 change the direction of the positive first-order diffracted radiation 95. A light detection unit  
20 107 detects the interference 89 of the two diffracted radiation signals to provide output signals 85. A signal processor 109 determines any misalignment between the structures from the output signals 85, preferably by comparing the output signals 85 to a reference signal. The output signals 85 contain information related to phase difference.

25 In one embodiment, phase shift interferometry is used to determine misalignment. The phase modulator 129 shifts the phase of positive first-order diffracted radiation 95. This phase shift of the positive first-order diffracted radiation 95 allows the signal processor 109 to use a simple algorithm to calculate the phase difference between the phase for the positive first-order diffracted radiation 95 and the  
30 phase for the negative first-order diffracted radiation 93.



Differential intensity and differential polarization angle can also be determined using optical system 120. The multi-aperture shutter 131 operates in three modes. The first mode allows both the positive first-order diffracted radiation 95 and the negative first-order diffracted radiation 93 to pass through. In this mode, differential phase is determined, as discussed above. The second mode allows only the positive first-order diffracted radiation 95 to pass through. In this mode, the intensity and polarization angle for the positive first-order diffracted radiation 95 can be determined, as discussed above. The third mode allows only the negative first-order diffracted radiation 93 to pass through. In this mode, the intensity and polarization angle for the negative first-order diffracted radiation 93 can be determined, as discussed above.

To determine differential intensity, the multi-aperture shutter 131 is operated in the second mode to determine intensity for positive first-order diffracted radiation 95 and then in the third mode to determine intensity for negative first-order diffracted radiation 93, or vice versa. The differential intensity is then calculated by subtracting the intensity of the negative first-order diffracted radiation 93 from the intensity of the positive first-order diffracted radiation 95. The signal processor 109 determines misalignment from the differential intensity.

In one embodiment, the differential intensity is measured at different incident polarization angles. The measurements result in a large set of data points, which, when compared to a reference signal, provide a high accuracy in the determined value of the misregistration.

To determine differential polarization angle, the multi-aperture shutter 131 is operated in the second mode to determine polarization angle for positive first-order diffracted radiation 95 and then in the third mode to determine polarization angle for negative first-order diffracted radiation 93, or vice versa. The differential polarization angle is then calculated by subtracting the polarization angle of the negative first-order diffracted radiation 93 from the polarization angle of the positive first-order diffracted radiation 95. The signal processor 109 determines misalignment from the differential polarization angle.

The imaging and focusing of the optical system 120 is verified using the vision and pattern recognition system 115 in the same way as the imaging and focusing of the optical system 110 is in Fig. 10. In one embodiment, the beam splitter 113 splits off radiation 89 to reference light detection unit 137, which detects  
5 fluctuations of the light source 101. The reference light detection unit 137 communicates information 86 concerning intensity fluctuation of source 101 to the signal processing and computing unit 109. The signal processor 109 normalizes the output signal 85 using fluctuation information 86.

Optical systems 100, 110, 120 can be integrated with a deposition instrument  
10 200 to provide an integrated tool, as shown in Figs. 9b, 10b and 11b. The deposition instrument 200 provides the overlying or interlaced periodic structures on wafer 91 in step 301. Optical systems 100, 110, 120 obtains misalignment information from the wafer 91 in step 302. The signal processor 109 of optical systems 100, 110, 120 provides the misalignment to the deposition tool 200 in step 303. The deposition tool  
15 uses the misalignment information to correct for any misalignment before providing another layer or periodic structure on wafer 91 in step 301.

Optical systems 100, 110, 120 are used to determine the misalignment of overlying or interlaced periodic structures. The source providing polarized incident radiation beam illuminates the first periodic structure 13 and the second periodic  
20 structure 15. Diffracted radiation from the illuminated portions of the overlying or interlaced periodic structures are detected to provide an output signal 85. The misalignment between the structures is determined from the output signal 85. In a preferred embodiment, the misalignment is determined by comparing the output signal 85 with a reference signal, such as a reference signal from a calibration wafer  
25 or a database, compiled as explained below.

The invention relates to a method for providing a database to determine misalignment of overlying or interlaced periodic structures. The misalignment of overlying or interlaced periodic structures and structure parameters, such as thickness, refractive index, extinction coefficient, or critical dimension, are provided to calculate  
30 data related to radiation diffracted by the structures in response to a beam of radiation. The data can include intensity, polarization angle, or phase information. Calculations

- can be performed using known equations or by a software package, such as Lambda SW, available from Lambda, University of Arizona, Tuscon, Arizona, or Gsolver SW, available from Grating Solver Development Company, P.O. Box 353, Allen, Texas 75013. Lambda SW uses eigenfunctions approach, described in P. Sheng, R. S. Stepleman, and P. N. Sandra, Exact Eigenfunctions for Square Wave Gratings: Applications to Diffraction and Surface Plasmon Calculations, Phys.Rev. B, 2907-2916 (1982), or the modal approach, described in L. Li, A Modal Analysis of Lamellar Diffraction Gratings in Conical Mountings, J. Mod. Opt. 40, 553-573 (1993). Gsolver SW uses rigorous coupled wave analysis, described in M. G. Moharam and T. K. Gaylord, Rigorous Coupled-Wave Analysis of Planar-Grating Diffraction, J. Opt. Soc. Am. 73, 1105-1112 (1983). The data is used to construct a database correlating the misalignment and the data. The overlay misregistration of a target can then be determined by comparing the output signal 85 with the database.

Figs. 12-24 were generated through computer simulations using either the Lambda SW or the Gsolver SW. Figs. 12a and 12b are graphical plots illustrating the ellipsometric parameters obtained using an overlying target of Fig. 2a with the optical system of Fig. 9a. The calculations were performed using the Lambda SW. The overlying target used in the measurement comprises first periodic structure 13 and the second periodic structure 15 made of resist gratings having 1  $\mu\text{m}$  depth on a silicon substrate. The depth of the first periodic structure 13 and the second periodic structure 15 is 0.5  $\mu\text{m}$ , and the pitch is 0.8  $\mu\text{m}$ . The first selected width CD1 for the first periodic structure 13 is 0.4  $\mu\text{m}$ , and the second selected width CD2 for the second periodic structure 15 is 0.2  $\mu\text{m}$ . The incident beam in this embodiment was TE polarized. These target parameters and the overlay misregistration were inputted into the Lambda SW to obtain ellipsometric parameter values. The ellipsometric parameter values were obtained for zero-order diffracted radiation using an incident radiation beam 81 at an angle of  $25^\circ$  to the wafer surface. The ellipsometric parameters,  $\text{Tan}[\Psi]$  and  $\text{Cos}[\Delta]$ , were plotted as a function of the wavelengths in the spectral range 230 to 400 nanometers. The ellipsometric parameters are defined as:

(3)

$$\tan \Psi = \frac{|r_p|}{|r_s|}$$

where  $r_p$  and  $r_s$  are the amplitude reflection coefficients for the p(TM) and s(TB) polarizations, and

5

(4)

$$\Delta = \phi_p - \phi_s$$

where  $\phi_p$  and  $\phi_s$  are the phases for the p(TM) and s(TB) polarizations. Results were obtained for different values of overlay misregistration  $d_2 - d_1$  varying from -15 nanometers to 15 nanometers in steps of 5 nanometers. The variations for  $\tan[\Psi]$  and  $\cos[\Delta]$  show sensitivity to the misregistration in the nanometer scale. To get more accurate results, first-order diffracted radiation is detected using normal incident radiation, as in Figs. 13-14.

Figs. 13 and 14 are graphical plots illustrating the differential intensity obtained using overlying targets of Fig. 2a and an optical system detecting first-order diffracted radiation using normal incident radiation. The calculations were performed using Gsolver SW. The first periodic layer 13 is etched silicon, while the second periodic layer 15 is resist. The overlay misregistration and target parameters were inputted into Gsolver SW to obtain the differential intensity in Figs. 13 and 14. Fig. 13 shows the normalized differential intensity between the positive and negative first-order diffracted radiation as a function of overlay misregistrations. The differential intensity is defined as:

(5)

$$DS = \frac{R_{+1} - R_{-1}}{R_{+1} + R_{-1}} \%$$

where  $R_{+1}$  is the intensity of the positive first-order diffracted radiation and  $R_{-1}$  is the intensity of the negative first-order diffracted radiation. The different curves in Fig.

13 correspond to the different incident polarization angles ( $0^\circ$ ,  $50^\circ$ ,  $60^\circ$ ,  $74^\circ$ ,  $80^\circ$ , and  $90^\circ$ ) of the incident linearly polarized light relative to the plane of incidence. The polarization angle  $\alpha$  is defined as:

(6)

5

$$\alpha = \arctan\left(\frac{|E_s|}{|E_p|}\right)$$

where  $E_s$  is the field component perpendicular to the plane of incidence, which for normal incidence is the Y component in the XY coordinate system, and  $E_p$  is the field component parallel to the plane of incidence, which for normal incidence is the X component. Polarization scans from incident polarization angles of  $0^\circ$  to  $90^\circ$  were performed to generate the graphical plots in Figs. 13 and 14. Fig. 14 shows the differential intensity as a function of incident polarization angle at different overlay misregistration (-50 nm, -35 nm, -15 nm, 0 nm, 15 nm, 35 nm, and 50nm). Fig. 14 shows that there is a neutral polarization angle, defined as an incident polarization angle where the differential intensity is equal to zero for all overlay misregistration. Figs. 13 and 14 illustrate the high sensitivity of differential intensity to the overlay misregistration and the linear behavior of differential intensity with the overlay misregistration. They also show that the differential intensity is zero at zero overlay misregistration for any polarization angle. Similar graphical plots were obtained at different wavelengths. Fig. 15 shows the mean square error ("MSE") variation with the overlay misregistration. The MSE exhibits linearity and sensitivity of approximately 0.6 per one nanometer overlay misregistration.

Figs. 16 and 17 are graphical plots, using the same target with different structure parameters and the same optical system as the ones in Figs. 13 and 14. However, the calculations were performed using the Lambda SW, instead of the Gsolver SW. The kinks or the deviations from the monotonicity of the curves at certain points in Figs. 16 and 17 are believed to be due to numerical instabilities frequently known to occur in the use of the Lambda SW. The overlay misregistration and the target parameters were inputted into Lambda SW to obtain differential polarization angle and differential phase in Figs. 16 and 17, respectively. Fig. 16

shows the variation of the difference between the polarization angles of the positive and negative first-order diffracted radiation as a function of overlay misregistration for different incident polarization angles ( $0^\circ$ ,  $5^\circ$ ,  $15^\circ$ ,  $30^\circ$ ,  $45^\circ$ ,  $60^\circ$ , and  $90^\circ$ ). Fig. 17 shows the variation of the difference between the phase angles of the positive and negative first-order diffracted radiation. The phase angle here represents the phase difference between the p and s polarized components of the diffracted light.

Figs. 16 and 17 also illustrate the high sensitivity of differential polarization angle and differential phase, respectively, to the overlay misregistration and the linear behavior of differential polarization angle and differential phase, respectively, when plotted against the overlay misregistration. They also show that the differential polarization angle and differential phase is zero at zero overlay misregistration for any polarization angle. However, Fig. 17 shows that the phase difference does not depend on incident polarization. In one embodiment, the difference between the polarization angles, as shown in Fig. 16, is easily measured with an analyzer at the output, while the phase difference, as shown in Fig. 17, is measured with interferometry. In another embodiment, the differential polarization angle and the differential phase is derived from ellipsometric parameters.

Similar results were obtained using the overlying targets in Figs. 4a and 4b. However, for the particular target in Fig. 4a, there was no neutral polarization angle in the line on line configuration, where the second periodic structure 15 is centered on the first periodic structure 13. The line on space configuration, where the second periodic structure 15 is centered on the spaces between the first periodic structure 13, did exhibit a neutral polarization angle. These results show that the neutral polarization angle apparently has a complicated dependence on the structure parameters.

Figs. 18-19 and 21-22 are graphical plots illustrating the intensity of the zero-order diffracted radiation 83, as shown in Fig. 9a, for interlaced gratings, as shown in Fig. 6. Table 1 summarizes the parameters used in the calculations by the Gsolver SW.

Table 1: Structure parameters used in the simulations

Parameter	Data76	Data0
h1	850 nm	850 nm
h2	850 nm	850 nm
h3	600 nm	600 nm
Pitch (P)	1000 nm	2000 nm
CD1	150 nm	200 nm
CD2	300 nm	600 nm
CD3	150 nm	200 nm
Incidence angle ( $\theta$ )	76°	0
Azimuth angle ( $\phi$ )	0	0
Wavelength ( $\lambda$ )	670 nm	500 nm

The incidence angle is 76° in the Data76 configuration, and the incidence angle is 0° (normal) in the Data0 configuration.

5 Figs. 18-20 were derived using the Data76 configuration. Fig. 18 shows the intensity of the zero-order diffracted radiation versus the overlay misregistration at different polarization angles (0° to 90° in steps of 15°). Within a range of 140 nm, the changes are monotonic with the overlay misregistration. The point where all the curves cross is at an overlay misregistration value of 50 nm, rather than zero. At an  
10 overlay misregistration value of 50 nm, the structure is effectively most symmetric. In contrast, in an overlying target as in Fig. 2a, the structure is most symmetric at zero overlay misregistration. Fig. 19 shows the dependence of the intensity of the zero-order diffracted radiation on the incident polarization angle at different overlay misregistrations (-50 nm, -15 nm, 0 nm, 20 nm, 40 nm, 60 nm, 80 nm, 100 nm, and  
15 130 nm). Unlike with the differential intensity of the first-order diffracted radiation, there is not a neutral polarization angle where the differential intensity is zero for different overlay misregistration. However, there is a quasi-neutral polarization angle where most of the curves for different misregistration cross. Fig. 20 shows the MSE variation as a function of overlay misregistration. Figs. 18 and 19 show the high  
20 sensitivity of the intensity of zero-order diffracted radiation to the overlay sign for a configuration using incident radiation having an oblique angle of incidence on interlaced gratings. They also show the linear behavior of the intensity when plotted against the overlay misregistration.

Figs. 21-23 were derived using the Data0 configuration. Fig. 21 shows the  
25 intensity of the zero-order diffracted radiation versus the overlay misregistration at

different polarization angles ( $0^\circ$ ,  $40^\circ$ ,  $65^\circ$ , and  $90^\circ$ ). Fig. 22 shows the dependence of the intensity of the zero-order diffracted radiation on the incident polarization angle at different overlay misregistrations (-140 nm, -100 nm, -50 nm, 0 nm, 50 nm, and 100 nm). Fig. 23 shows the MSE variation as a function of overlay misregistration. Figs. 21 and 22 show the high sensitivity of the intensity of zero-order diffracted radiation to the overlay sign for a configuration using normal incident radiation on interlaced gratings. They also show the linear behavior of the intensity when plotted against the overlay misregistration.

Fig. 24 is a graphical plot generated by the Gsolver SW illustrating the determination of misalignment from the neutral polarization angle. As shown in Fig. 14, the differential intensity equals zero independent of the overlay misregistration at the neutral polarization angle. However, the slope of the differential intensity varies with overlay misregistration. Fig. 24 shows the slope near the neutral polarization angle as a function of overlay misregistration. Fig. 24 shows linear behavior of the slope versus the overlay misregistration with a slope of 0.038% per 1 nm overlay misregistration. An advantage of the slope measurement technique is the reduction of the number of parameters that need to be determined. Another advantage is the decreased polarization scanning needed. In Fig. 14, a polarization scan using incident polarization angles from  $0^\circ$  to  $90^\circ$  is performed. In contrast, using the slope measurement technique in one embodiment, the derived signal is compared with the reference signal for polarization angles within about five degrees of the neutral polarization angle. Thus, the method of detecting misalignment is faster when using the slope measurement technique. Another embodiment of the invention is the use of the slope measurement technique for the quasi-neutral polarization angle.

Misalignment of overlying or interlaced periodic structures can be determined using the database in a preferred embodiment. The source providing polarized incident radiation illuminates the first periodic structure 13 and the second periodic structure 15. Diffracted radiation from the illuminated portions of the overlying or interlaced periodic structures are detected to provide an output signal 85. The output signal 85 is compared with the database to determine the misalignment between the overlying or interlaced periodic structures.



In another embodiment, misalignment of overlying or interlaced periodic structures is determined using the slope measurement technique. A neutral polarization angle or quasi-neutral polarization angle is provided. The derived signal is compared with the reference signal near the neutral polarization angle or the quasi-neutral polarization angle to determine misalignment of the overlying or interlaced periodic structures.

While the invention has been described above by reference to various embodiments, it will be understood that changes and modifications may be made without departing from the scope of the invention, which is to be defined only by the appended claims and their equivalent. All references referred to herein are incorporated by reference.

WHAT IS CLAIMED IS:

1. A target for measuring the relative positions between two layers of a device, said target comprising:  
5           a first periodic structure over a first layer of the device; and  
            a second periodic structure over a second layer of the device, said second periodic structure overlying or interlaced with said first periodic structure.
2. The target of claim 1, wherein the first periodic structure has a first  
10       selected width, and the second periodic structure has a second selected width, the second selected width being less than the first selected width.
3. The target of claim 1, wherein said second periodic structure extends  
15       further to an area where said first periodic structure does not extend.
4. The target of claim 1, wherein the first layer is etched silicon, and the  
      second layer is resist.
5. The target of claim 1, wherein said first periodic structure has a  
20       trapezoidal shape, the first layer is silicon dioxide, and the second layer is resist, the first layer and the second layer being separated by an uniform polysilicon layer.
6. The target of claim 1, wherein said first periodic structure is tungsten  
      and has a concave-trapezoidal shaped top, the first layer is oxide, and the second layer  
25       is resist, the first layer and the second layer being separated by an aluminum blanket.
7. The target of claim 1, further comprising unpatterned semiconductor,  
      metal, or dielectric layers deposited or grown on top of, underneath, or between the  
      first and the second layers.  
30
8. The target of claim 1, wherein a layer that is the topmost layer is resist.

9. The target of claim 1, wherein the first periodic structure has been exposed to radiation for patterning purposes of a semiconductor wafer.

10. The target of claim 1, further comprising:

5 a third periodic structure that is substantially perpendicular to said first periodic structure, said third periodic structure over the first layer, and

a fourth periodic structure that is substantially perpendicular to said second periodic structure, said fourth periodic structure over the second layer and overlying or interlaced with said third periodic structure.

10 11. The target of claim 1, wherein said first periodic structure has at least two interlaced grating lines having different periods, line widths or duty cycles.

12. The target of claim 1, wherein said second periodic structure has at  
15 least two interlaced grating lines having different periods, line widths or duty cycles.

13. A method for making a target, comprising:

placing a first periodic structure over a first layer of a device; and

20 placing a second periodic structure over a second layer of a device, wherein said second periodic structure is overlying or interlaced with said first periodic structure.

14. The method of claim 13, wherein said placing a second periodic structure includes placing said second periodic structure on an area to where said first  
25 periodic structure does not extend.

15. The method of claim 13, further comprising exposing the first periodic structure to radiation for patterning purposes of a semiconductor wafer.

30 16. The method of claim 13, further comprising:

placing a third periodic structure over the first layer, wherein said third periodic structure is substantially perpendicular to said first periodic structure; and

placing a fourth periodic structure over the second layer, wherein said fourth periodic structure is substantially perpendicular to said second periodic structure.

5           17. The method of claim 13, wherein said placing a first periodic structure includes placing at least two interlaced grating lines having different periods, line widths or duty cycles.

10           18. The method of claim 13, wherein said placing a second periodic structure includes placing at least two interlaced grating lines having different periods, line widths or duty cycles.

15           19. A method for providing a database to determine misalignment of overlying or interlaced periodic structures, comprising:

providing information related to thickness, refractive index, extinction coefficient, or critical dimension, and misalignment of periodic structures that overlie or interlace one another;

deriving from said information data related to radiation diffracted by the structures in response to a beam of radiation; and

20           constructing a database correlating the misalignment and the data.

20. The method of claim 19, further comprising calculating a differential intensity, a differential phase, or a differential polarization angle from the data.

25           21. A method for detecting misalignment of overlying or interlaced periodic structures, comprising:

illuminating the overlying or interlaced periodic structures with incident radiation;

30           detecting diffracted radiation from the illuminated portions of the overlying or interlaced periodic structures to provide an output signal; and

determining a misalignment between the structures from the output signal.

22. The method of claim 21, wherein said determining includes comparing the output signal with a reference signal.
23. The method of claim 22, wherein the reference signal comprises a  
5 database.
24. The method of claim 21, wherein the output signal contains information related to ellipsometric parameters.
- 10 25. The method of claim 21, wherein overlying or interlaced periodic structures has at least two interlaced grating lines having different periods, line widths or duty cycles; the incident radiation is incident on the structures at an oblique angle; and the diffracted radiation comprises zero-order diffraction.
- 15 26. The method of claim 21, wherein overlying or interlaced periodic structures has at least two interlaced grating lines having different periods, line widths or duty cycles; the incident radiation is incident on the structures at a normal angle; and the diffracted radiation comprises zero-order diffraction.
- 20 27. The method of claim 21, wherein the incident radiation is substantially normal, and the diffracted radiation comprises positive first-order diffraction and negative first-order diffraction.
- 25 28. The method of claim 21, further comprising calculating a derived signal from the output signal.
29. The method of claim 28, wherein the derived signal contains information related to intensity, phase, or polarization angle.
- 30 30. The method of claim 28, wherein the derived signal contains information related to differential intensity, differential phase, or differential polarization angle.

31. The method of claim 28, further comprising providing a neutral polarization angle or quasi-neutral polarization angle; and wherein said determining a misalignment includes determining a misalignment by comparing the derived signal with the reference signal near the neutral polarization angle or the quasi-neutral polarization angle.

32. The method of claim 31, wherein the derived signal is compared with the reference signal for polarization angles within about five degrees of the neutral polarization angle or the quasi-neutral polarization angle.

33. An apparatus for detecting misalignment of overlying or interlaced periodic structures, comprising:

a source providing polarized incident radiation beam to illuminate the overlying or interlaced periodic structures;

at least one analyzer collecting diffracted radiation from the structures;  
at least one detector detecting diffracted radiation collected by the analyzer to provide output signals; and

a signal processor determining any misalignment between the structures from the output signals.

34. The apparatus of claim 33, wherein the source provides incident radiation beam having an oblique angle of incidence to illuminate the overlying or interlaced periodic structures, and the detector detects zero-order diffraction.

35. The apparatus of claim 33, wherein the source provides a normal incident radiation beam to illuminate the overlying or interlaced periodic structures, and the detector detects zero-order diffraction.

36. The apparatus of claim 33, wherein the source includes a polarizer and a device causing relative rotational motion between the polarizer and the analyzer.

37. The apparatus of claim 33, wherein said at least one analyzer comprises a first analyzer collecting positive first-order diffracted radiation and a

second analyzer collecting negative first-order diffracted radiation; and said at least one detector comprises a first detector detecting positive first-order diffracted radiation, and a second detector detecting negative first-order diffracted radiation.

5           38. The apparatus of claim 37, wherein the signal processor calculates a derived signal from the output signals.

          39. The apparatus of claim 38, wherein the derived signal contains information related to a differential intensity, a differential phase, or a differential  
10       polarization angle.

          40. The apparatus of claim 38, wherein the source includes a polarizer and a device causing relative rotational motion between the polarizer and the analyzers.

15           41. The apparatus of claim 40, wherein the derived signal contains information related to a differential polarization angle or a phase difference derived from ellipsometric parameters.

          42. An apparatus for detecting misalignment of overlying or interlaced  
20       periodic structures, comprising:

          a source providing polarized incident radiation beam to illuminate the overlying or interlaced periodic structures;

          two analyzers collecting first-order diffracted radiation from the structures, the first-order diffracted radiation comprising a positive first-order  
25       diffraction and a negative first-order diffraction;

          a first device interfering the positive first-order diffraction and the negative first order diffraction from the analyzers to provide a combined diffracted radiation signal;

          a detector detecting the combined diffracted radiation signal to provide  
30       output signals; and

          a signal processor determining any misalignment between the structures from the output signals.

43. The apparatus of claim 42, wherein the output signal contains information related to phase difference between the positive first-order diffraction and the negative first-order diffraction.

5 44. An apparatus for making overlying or interlaced periodic structures and detecting misalignment between the overlying or interlaced periodic structures, comprising:

a deposition instrument to provide the overlying or interlaced periodic structures;

10 a source providing polarized incident radiation beam to illuminate the overlying or interlaced periodic structures;

at least one analyzer collecting diffracted radiation from the structures;

at least one detector detecting diffracted radiation collected by the analyzer to provide output signals; and

15 a signal processor determining any misalignment between the structures from the output signals and providing the misalignment to the deposition instrument.

45. The apparatus of claim 44, wherein the source provides an incident radiation beam having an oblique angle of incidence to illuminate the overlying or interlaced periodic structures, and the detector detects zero-order diffraction.

46. The apparatus of claim 44, wherein the source provides a normal incident radiation beam to illuminate the overlying or interlaced periodic structures, and the detector detects zero-order diffraction.

47. The apparatus of claim 44, wherein the source includes a polarizer and a device causing relative rotational motion between the polarizer and the analyzer.

30 ~~48.~~ The apparatus of claim 44, wherein said at least one analyzer comprises a first analyzer collecting positive first-order diffracted radiation and a second analyzer collecting negative first-order diffracted radiation; and said at least



one detector comprises a first detector detecting positive first-order diffracted radiation, and a second detector detecting negative first-order diffracted radiation.

49. The apparatus of claim 48, wherein the signal processor calculates a  
5 derived signal from the output signals.

50. The apparatus of claim 49, wherein the derived signal contains  
information related to a differential intensity, a differential phase, or a differential  
polarization angle.

10

51. The apparatus of claim 49, wherein the source includes a polarizer and  
a device causing relative rotational motion between the polarizer and the analyzers.

52. The apparatus of claim 51, wherein the derived signal contains  
15 information related to a differential polarization angle or a phase difference derived  
from ellipsometric parameters.

53. An apparatus for making overlying or interlaced periodic structures  
and detecting misalignment between the overlying or interlaced periodic structures,  
20 comprising:

a deposition instrument to provide the overlying or interlaced periodic  
structures;

a source providing polarized incident radiation beam to illuminate the  
overlying or interlaced periodic structures;

25 two analyzers collecting first-order diffracted radiation from the  
structures, the first-order diffracted radiation comprising a positive first-order  
diffraction and a negative first-order diffraction;

a first device interfering the positive first-order diffraction and the  
negative first order diffraction from the analyzers to provide a combined diffracted  
30 radiation signal;

a detector detecting the combined diffracted radiation signal to provide  
output signals; and

a signal processor determining any misalignment between the structures from the output signals and providing the misalignment to the deposition instrument.

- 5        54. The apparatus of claim 53, wherein the output signal contains information related to phase difference between the positive first-order diffraction and the negative first-order diffraction.

1/22

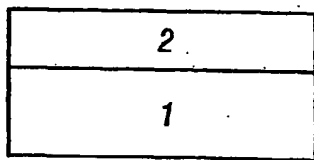


FIG. 1a

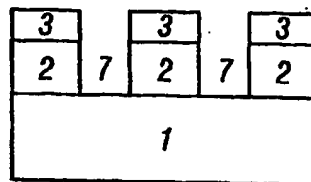


FIG. 1e

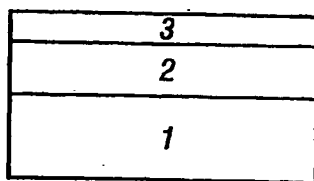


FIG. 1b

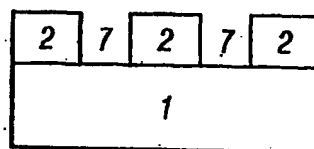


FIG. 1f

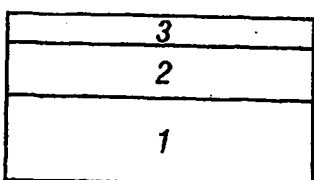
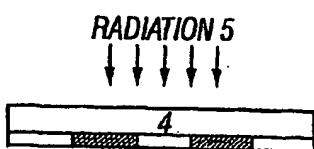


FIG. 1c

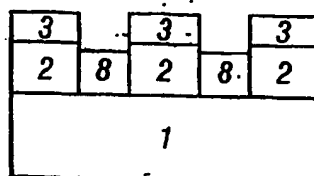


FIG. 1g

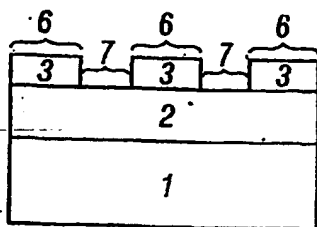


FIG. 1d

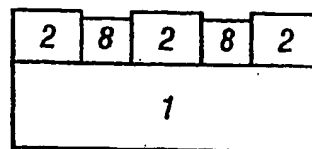


FIG. 1h

2/22

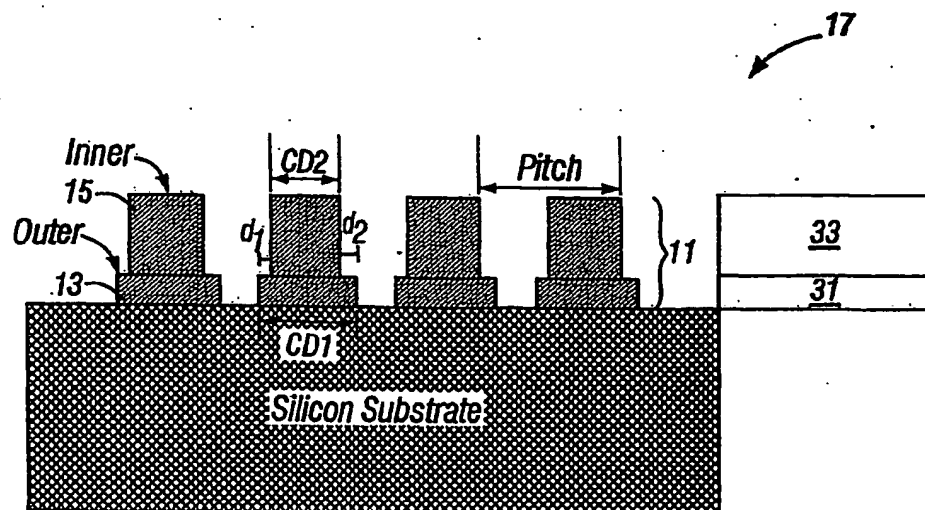


FIG. 2a

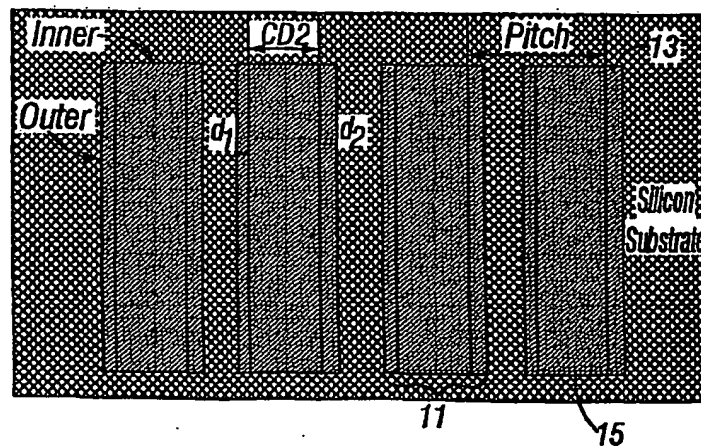


FIG. 2b

3/22

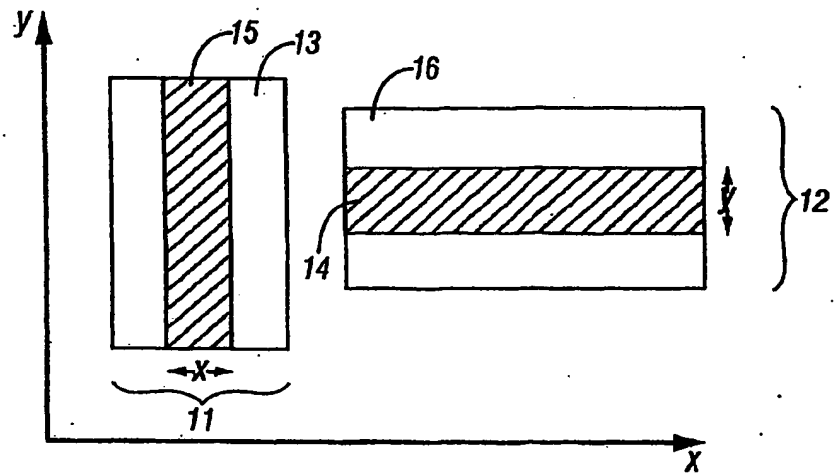


FIG. 2c

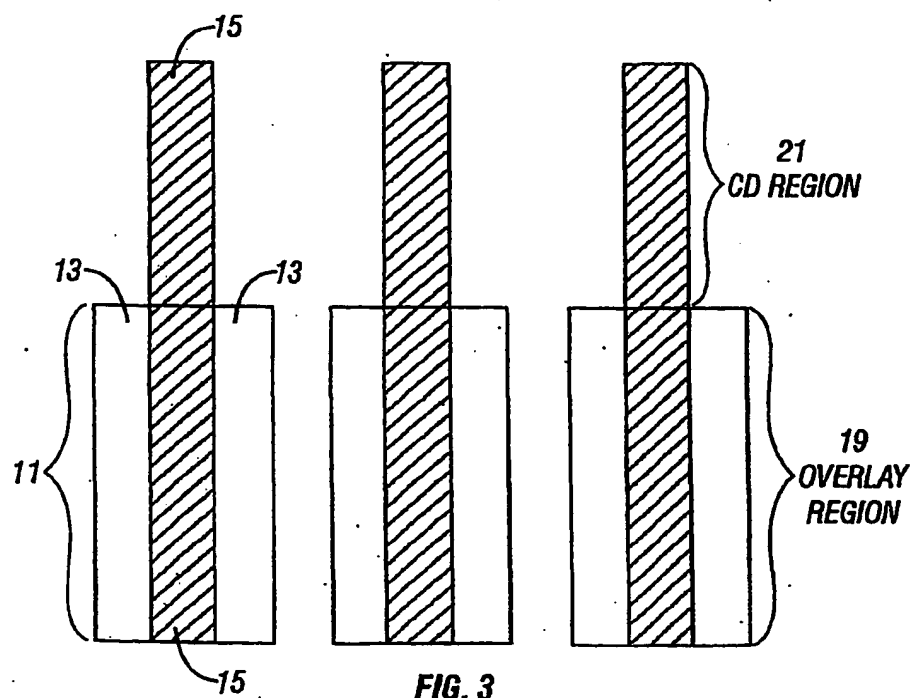


FIG. 3

4/22

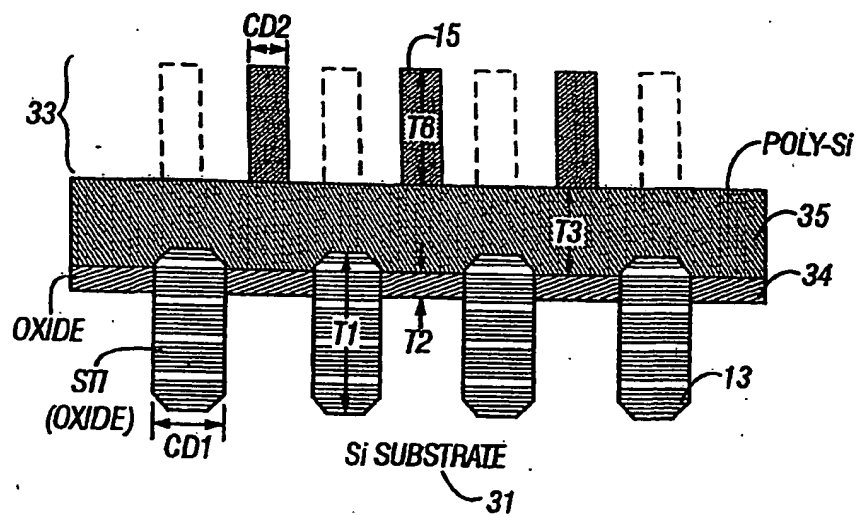


FIG. 4a

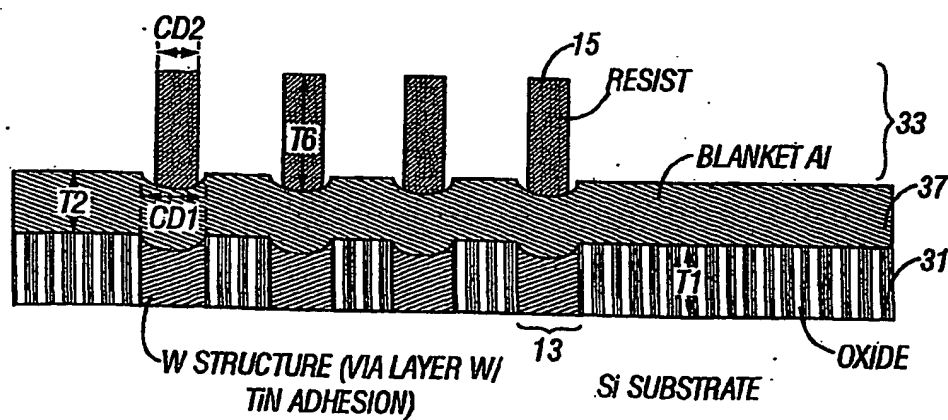


FIG. 4b

5/22

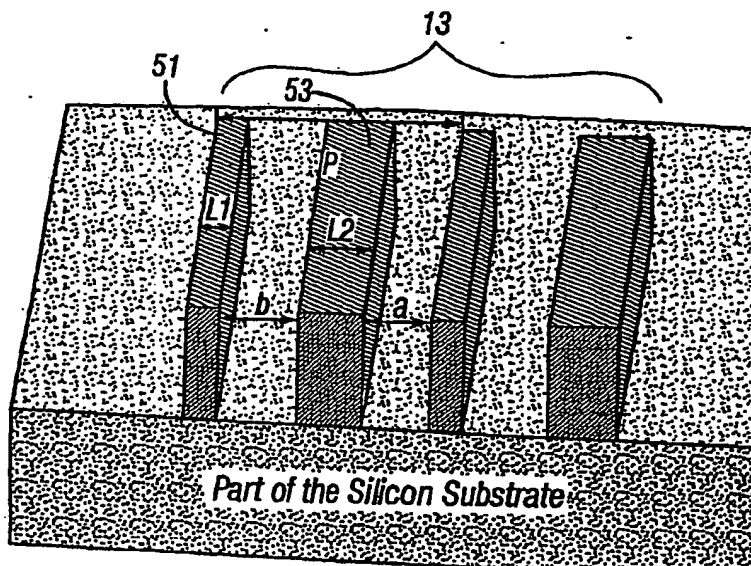


FIG. 5a

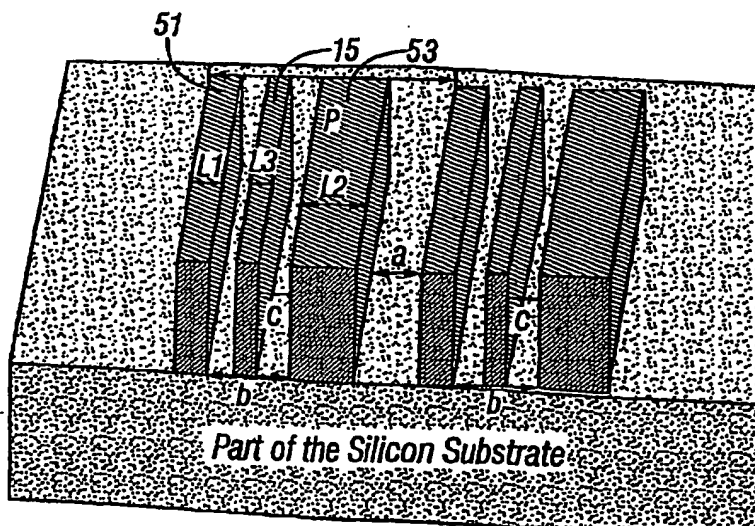


FIG. 5b

6/22

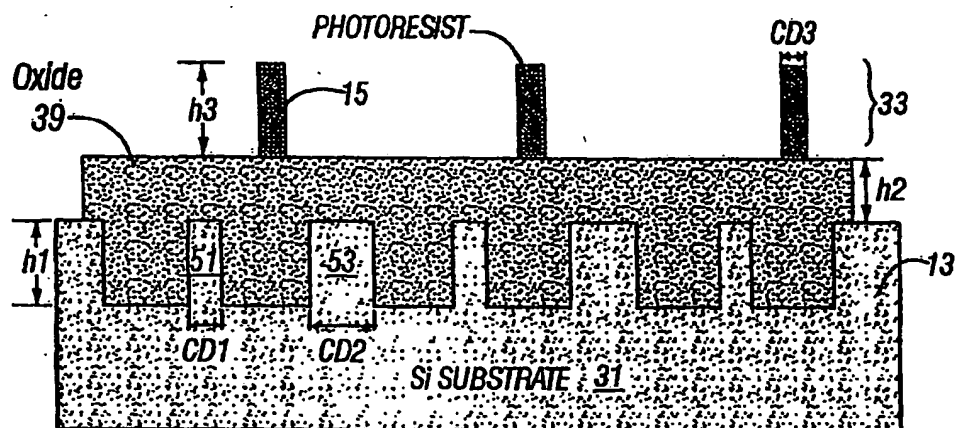


FIG. 6

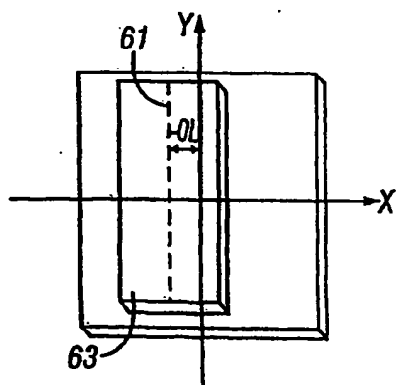


FIG. 7a

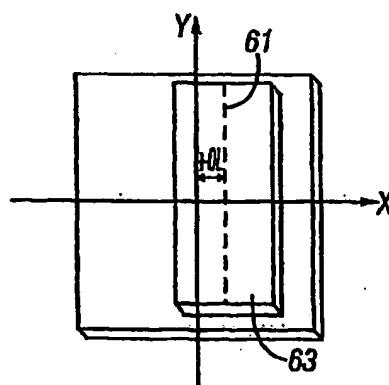


FIG. 7b



7/22

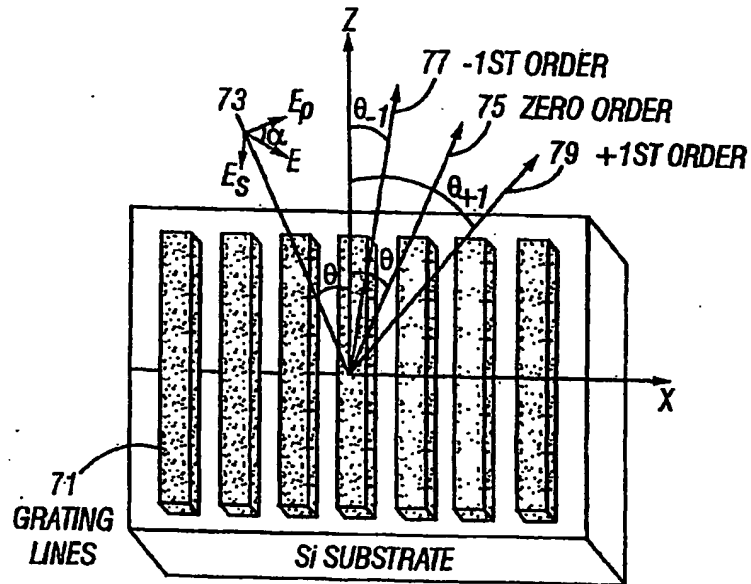


FIG. 8

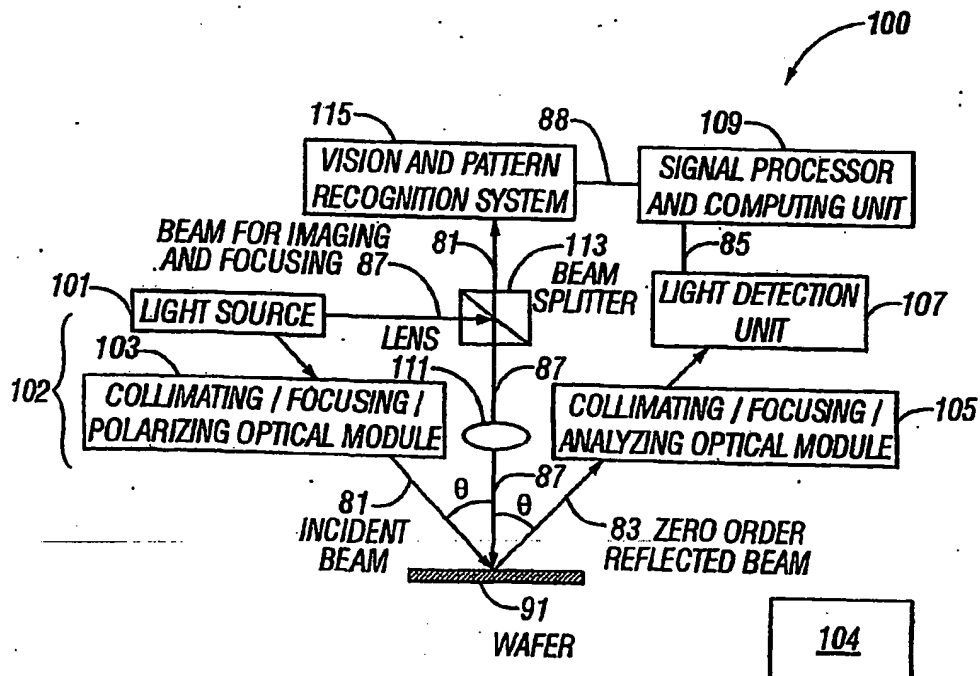


FIG. 9a

8/22

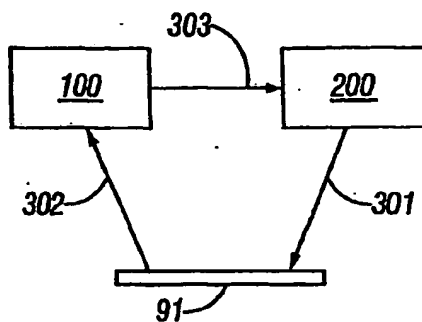


FIG. 9b

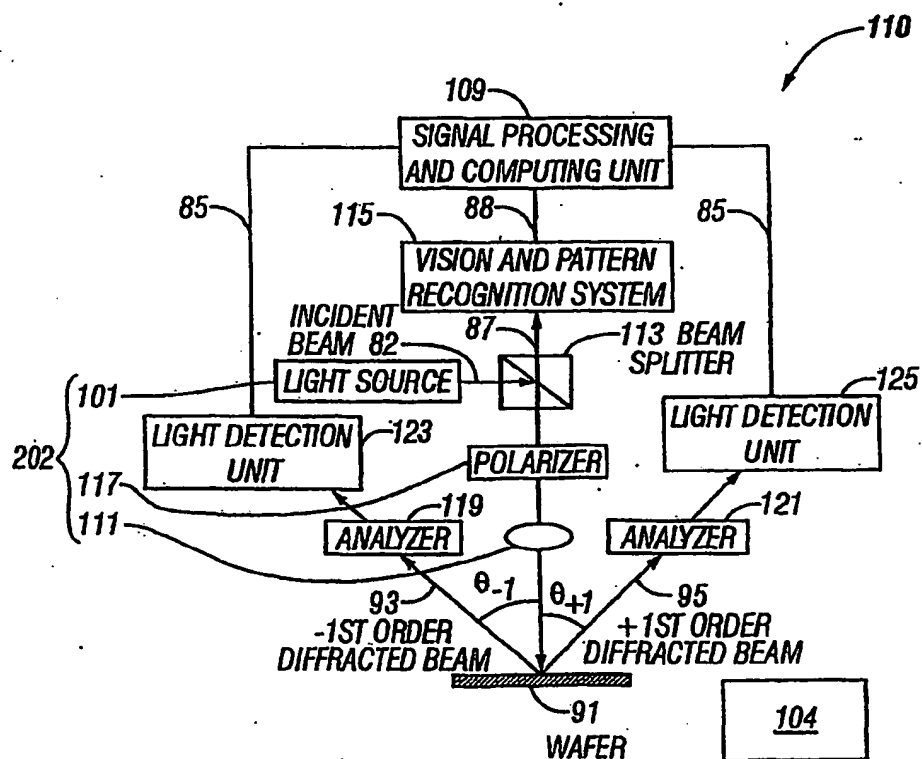


FIG. 10a

9/22

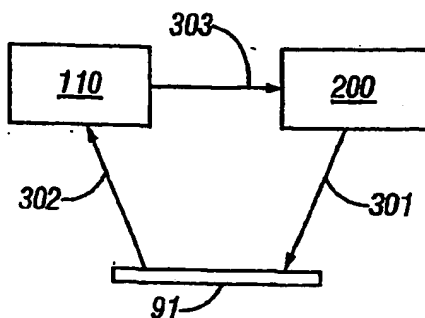


FIG. 10b

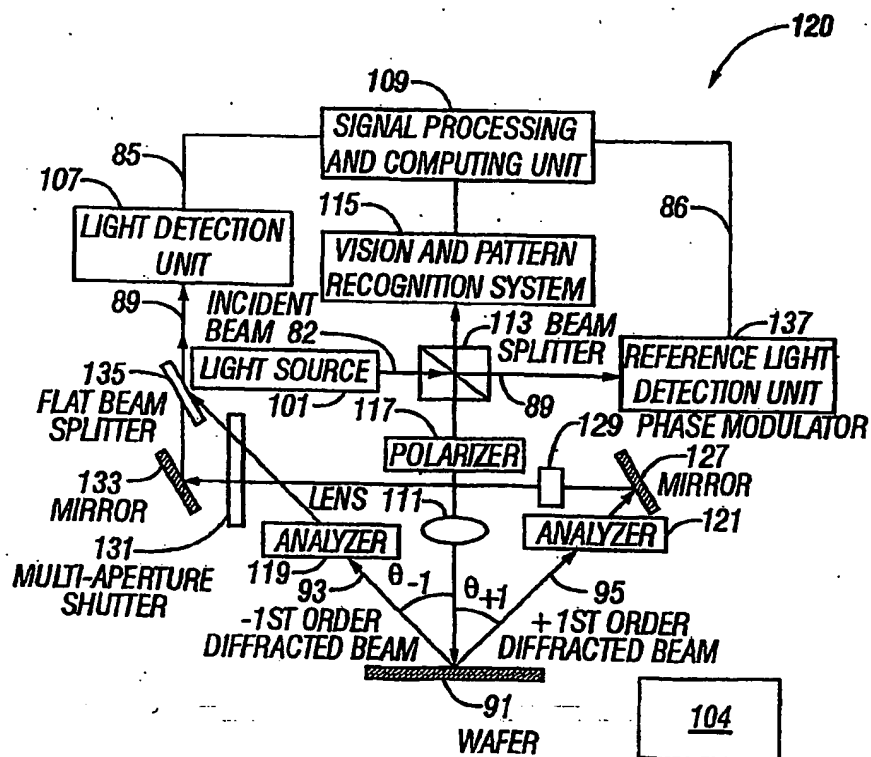


FIG. 11a

10/22

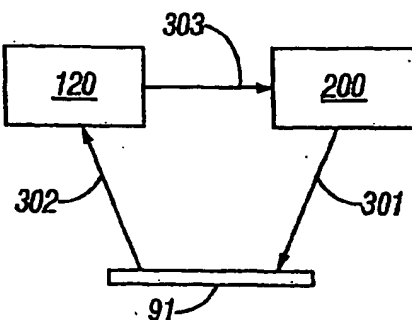


FIG. 11b

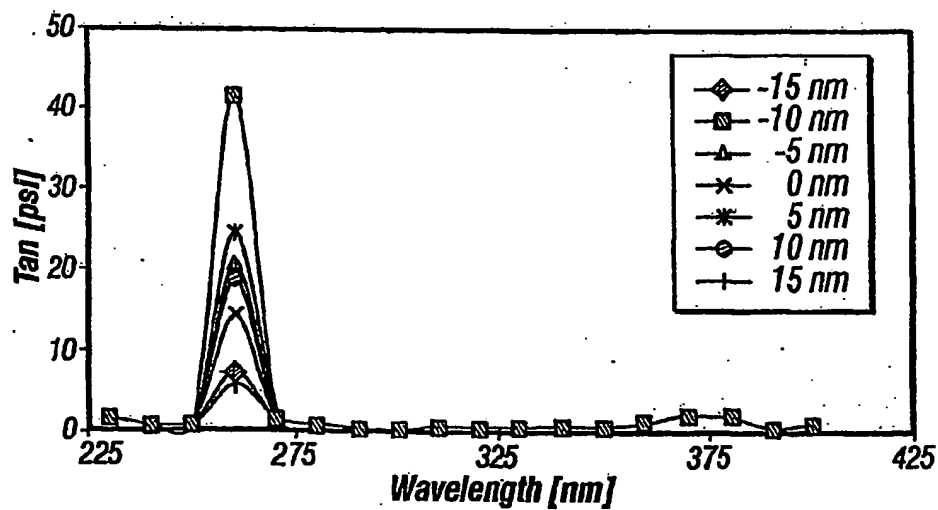


FIG. 12a

11/22

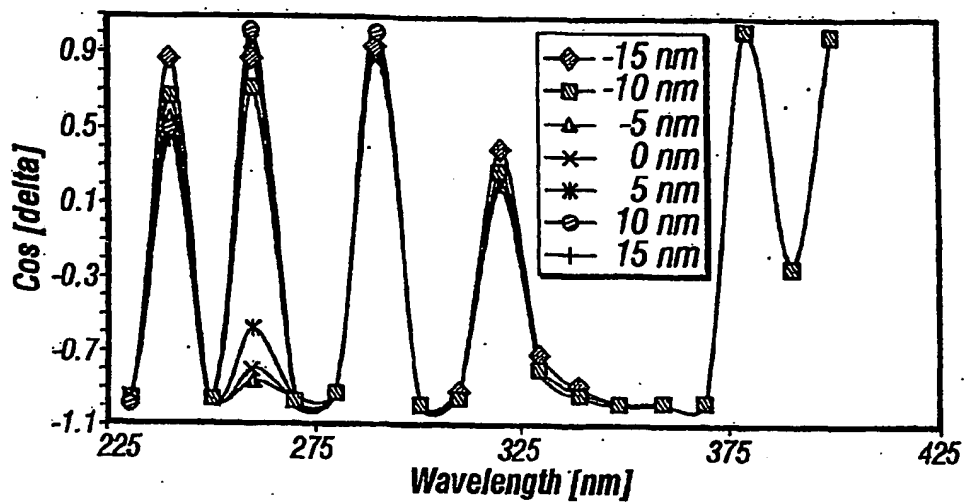


FIG. 12b

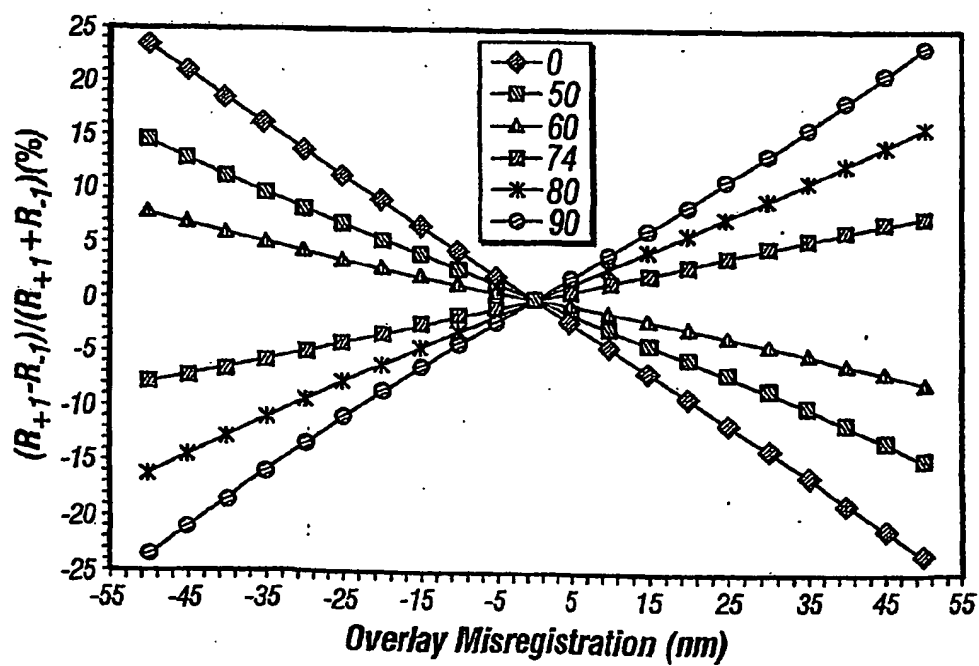
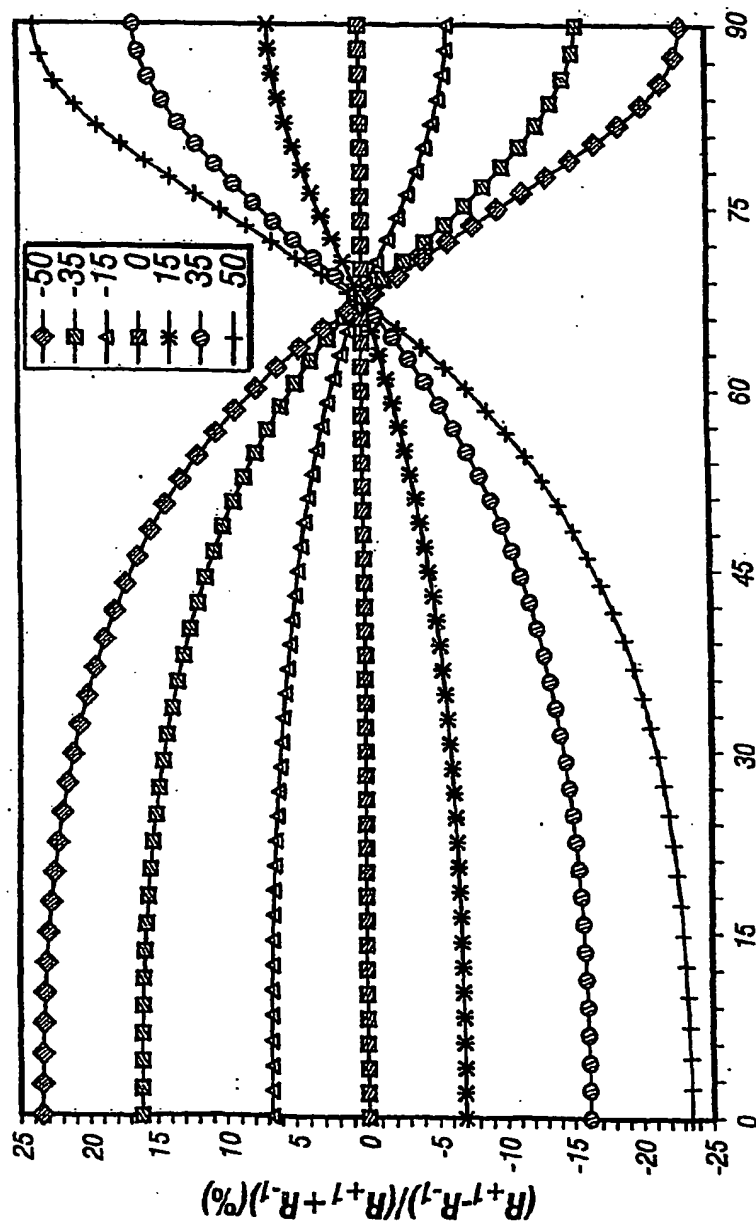


FIG. 13

12/22



Incident Polarization Angle

FIG. 14

13/22

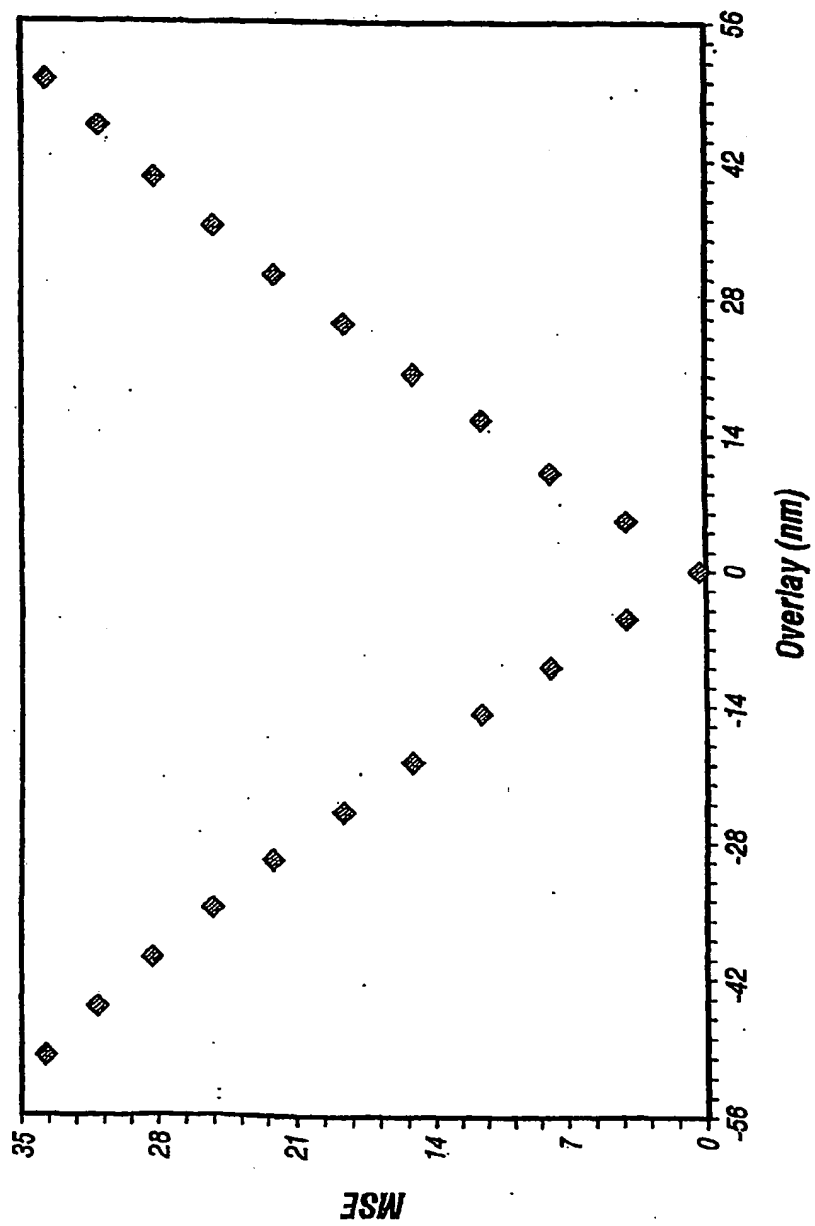
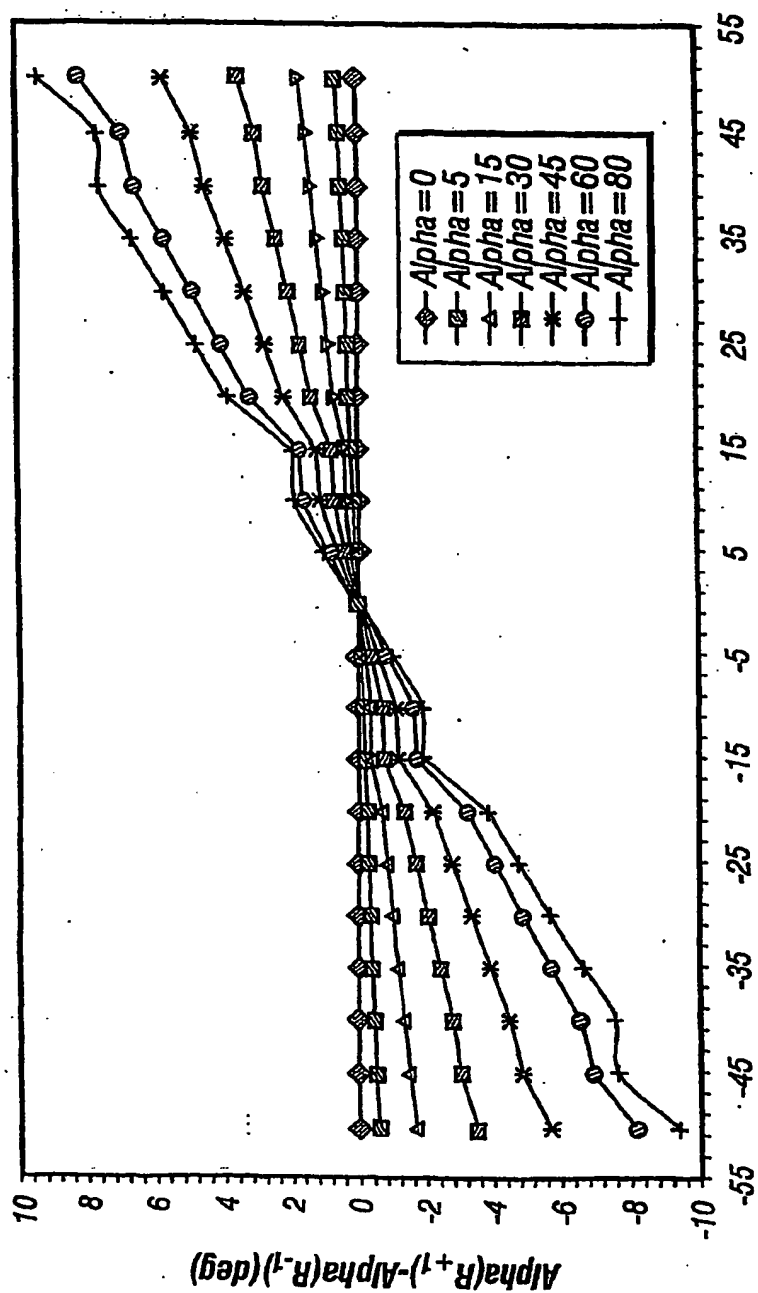


FIG. 15

14/22

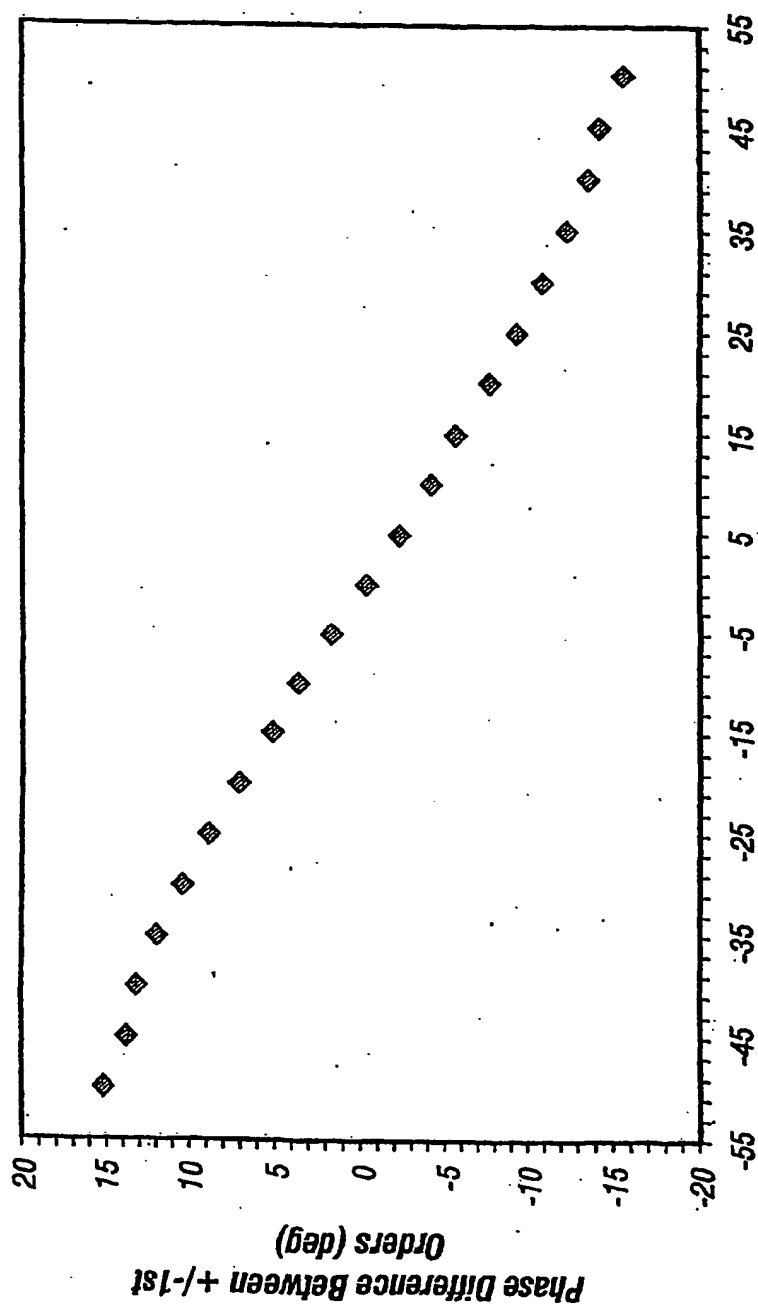


Overlay Misregistration (nm)

FIG. 16



15/22



Overlay Misregistration (nm)

FIG. 17

16/22

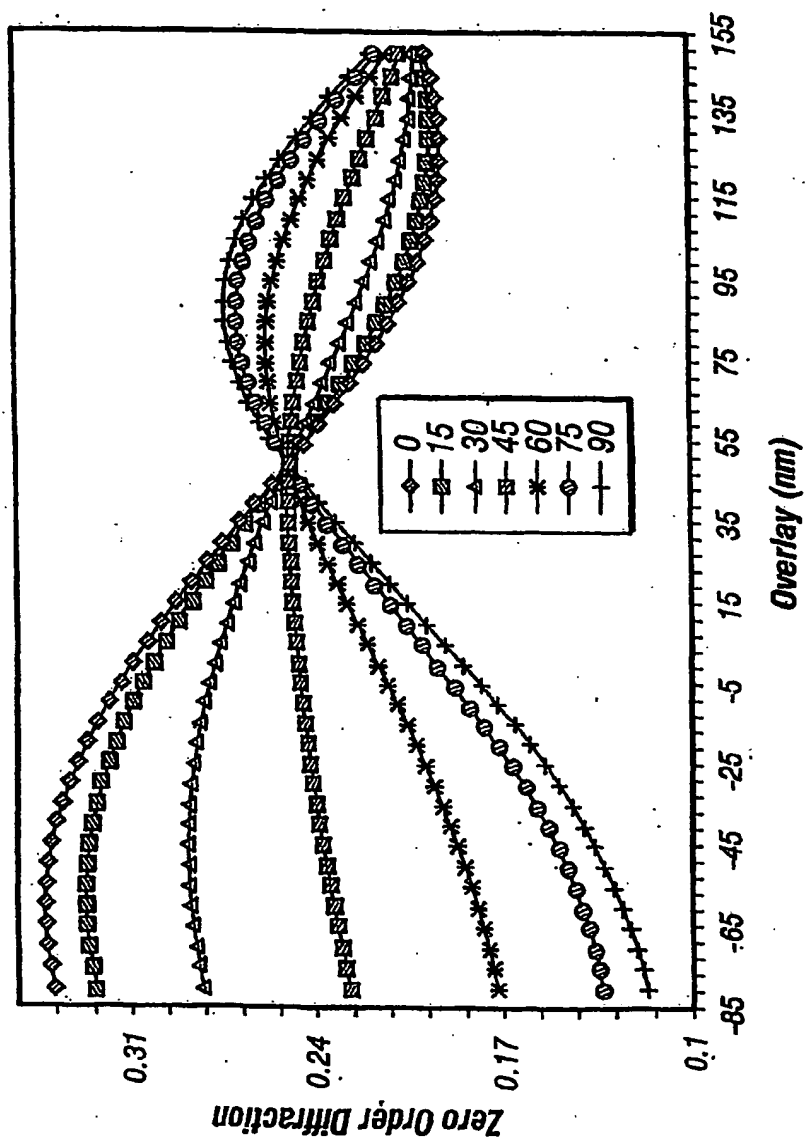


FIG. 18

17/22

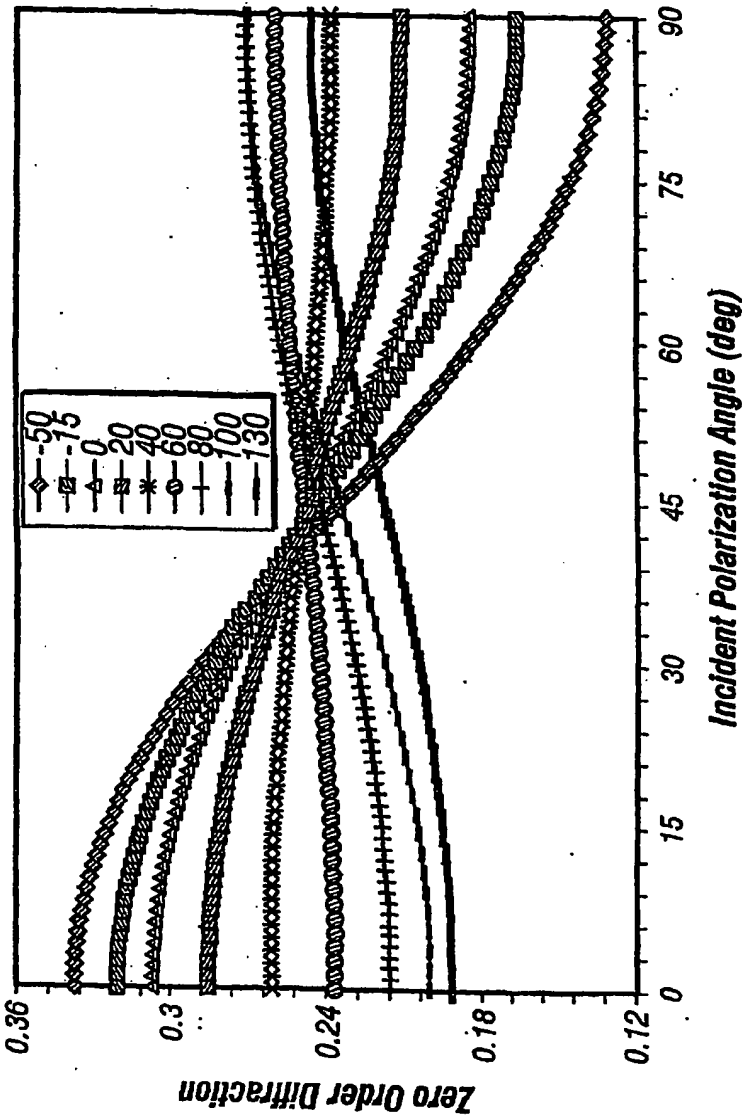


FIG. 19

18/22

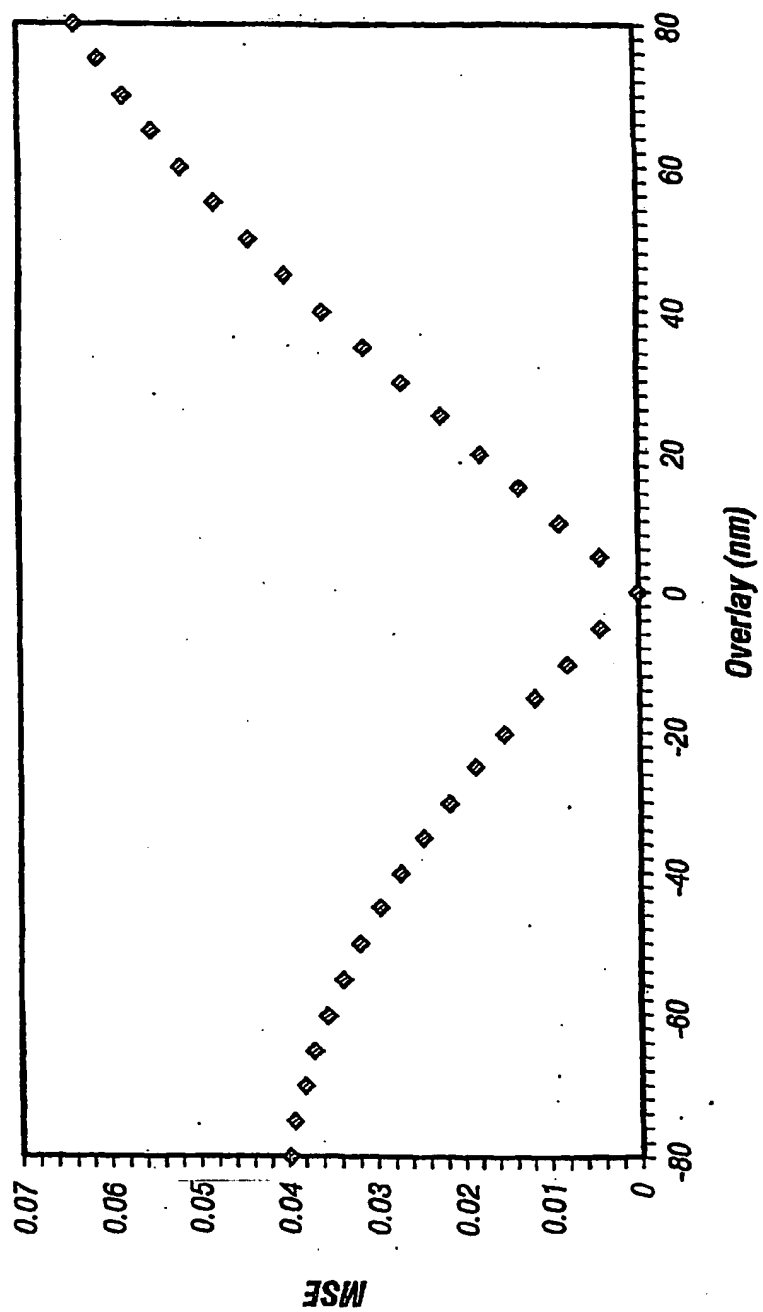


FIG. 20

19/22

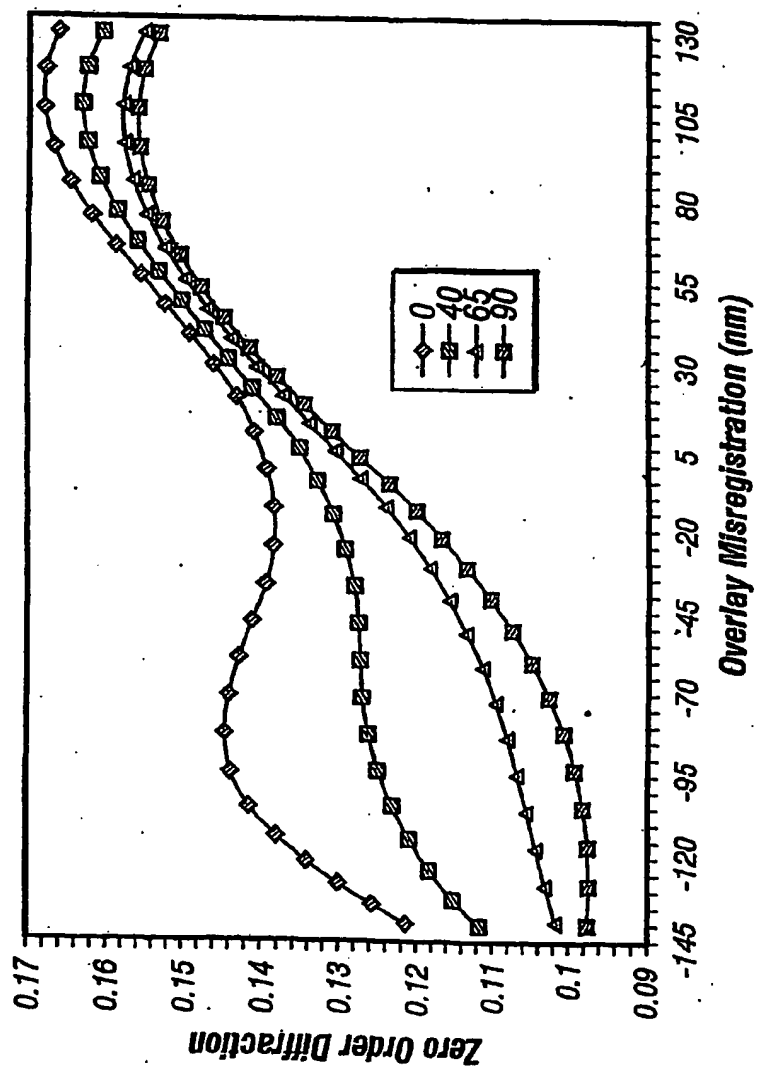


FIG. 21

20/22

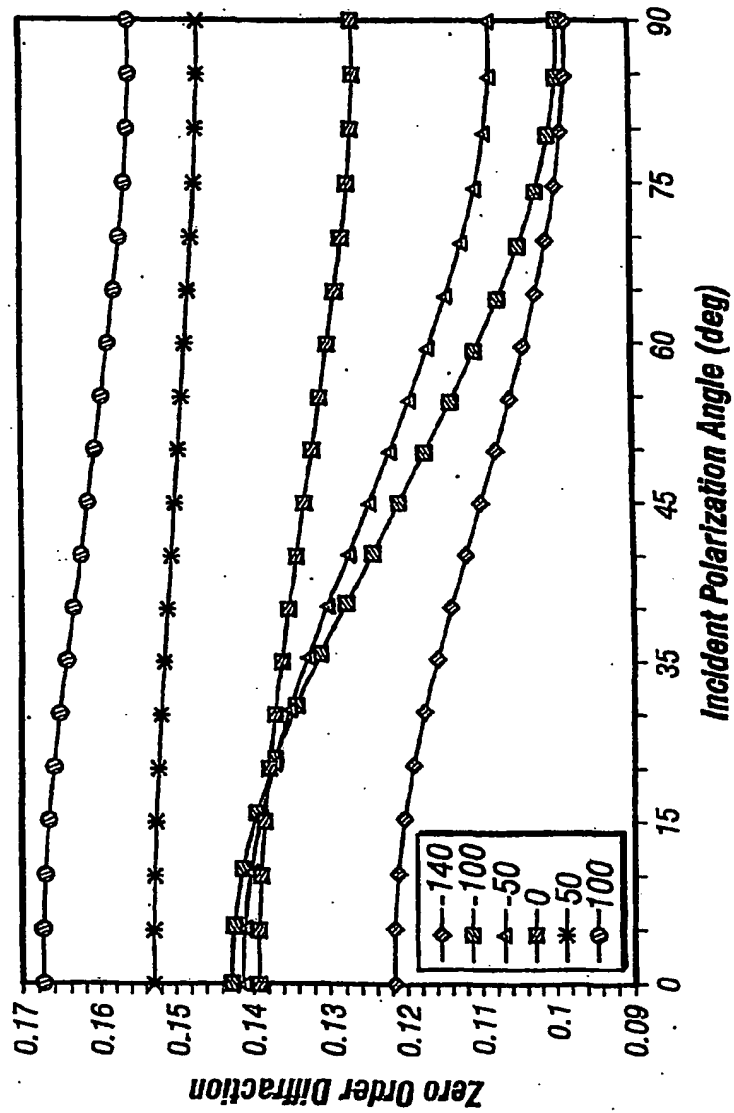


FIG. 22

21/22

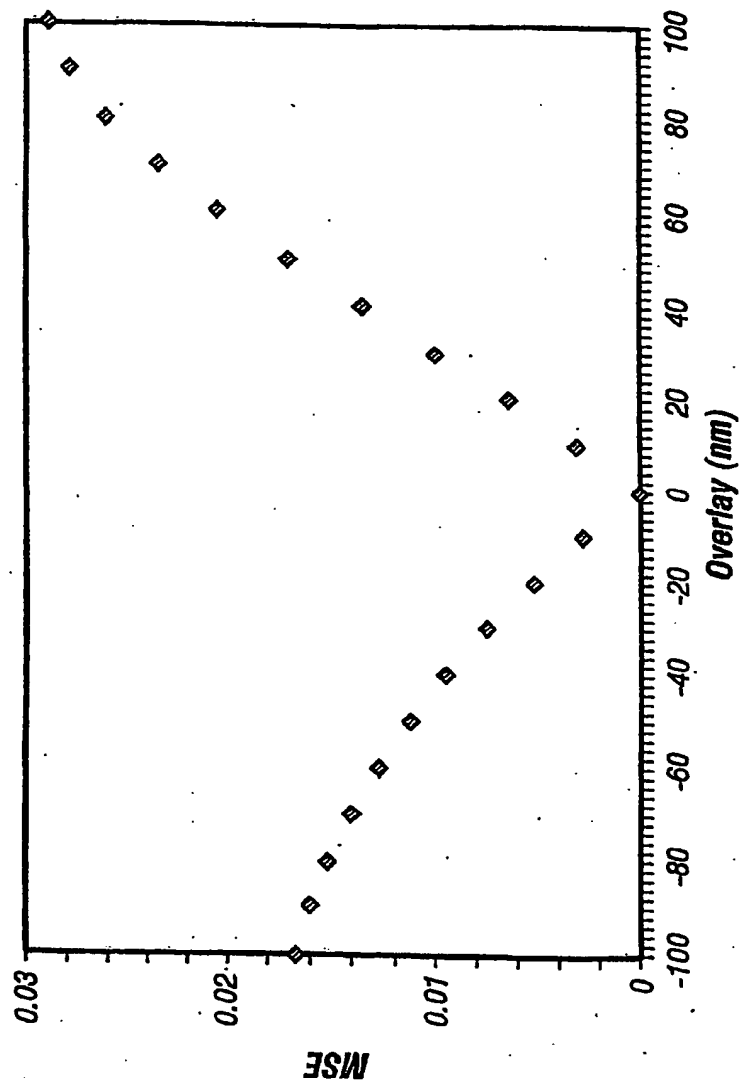


FIG. 23

22/22

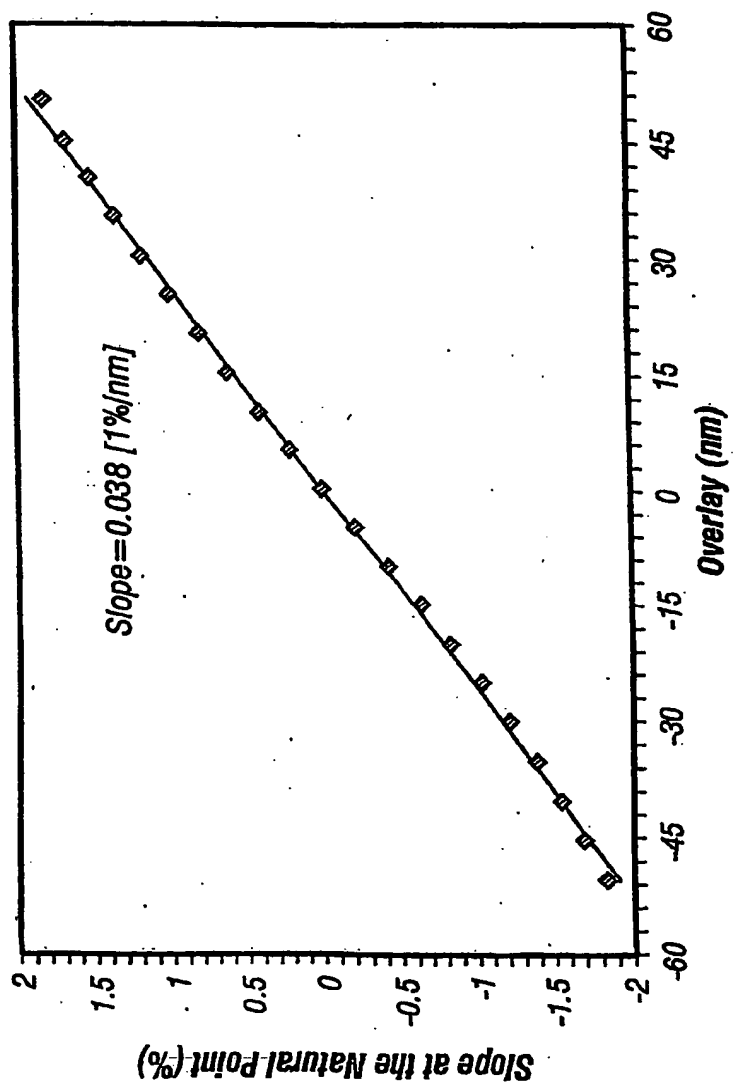


FIG. 24



## INTERNATIONAL SEARCH REPORT

International application No.

PCT/US02/11026

**A. CLASSIFICATION OF SUBJECT MATTER**

IPC(7) : G01B 11/00; G03F 9/00; G01N 21/86

US CL : 356/400-401; 250/548; 430/22

According to International Patent Classification (IPC) or to both national classification and IPC

**B. FIELDS SEARCHED**

Minimum documentation searched (classification system followed by classification symbols)

U.S. : 356/400-401; 250/548; 430/22

Documentation searched other than minimum documentation to the extent that such documents are included in the fields searched

Electronic data base consulted during the international search (name of data base and, where practicable, search terms used)  
Please See Continuation Sheet**C. DOCUMENTS CONSIDERED TO BE RELEVANT**

Category *	Citation of document, with indication, where appropriate, of the relevant passages	Relevant to claim No.
X — Y	US 6,079,256 A (BAREKET) 27 JUNE 2000 (27-06-2000), see entire document.	1-4, 8-18, 21-23, 25-30, 30, and 33-34
y	US 5,607,818 A (AKRAM et al.) 04 MARCH 1997 (04-03-1997), see entire document.	5-7, 19-20, 24, 31-31 5-7, 19-20, 24, and 31-32

☐ Further documents are listed in the continuation of Box C.☐ See patent family annex.

\* Special categories of cited documents:

"A" document defining the general state of the art which is not considered to be of particular relevance

"E" earlier application or patent published on or after the international filing date

"L" document which may throw doubts on priority claim(s) or which is cited to establish the publication date of another claim or other special reason (as specified)

"O" document referring to an oral disclosure, use, exhibition or other means

"P" document published prior to the international filing date but later than the priority date claimed

"T"

later document published after the international filing date or priority date and not in conflict with the application but cited to understand the principle or theory underlying the invention

"X"

document of particular relevance; the claimed invention cannot be considered novel or cannot be considered to involve an inventive step when the document is taken alone

"Y"

document of particular relevance; the claimed invention cannot be considered to involve an inventive step when the document is combined with one or more other such documents, such combination being obvious to a person skilled in the art

"A"

document member of the same patent family

Date of the actual completion of the international search

28 June 2002 (28.06.2002)

Date of mailing of the international search report

18 SEP 2002

Name and mailing address of the ISA/US

Commissioner of Patents and Trademarks  
Box PCT  
Washington, D.C. 20231

Facsimile No. (703)305-3230

Authorized officer

Zandra V. Smith

Telephone No. (703) 305-0536

Form PCT/ISA/210 (second sheet) (July 1998)

## ARTIFACT SHEET

Enter artifact number below. Artifact number is application number + artifact type code (see list below) + sequential letter (A, B, C ...). The first artifact folder for an artifact type receives the letter A, the second B, etc..

Examples: 59123456PA, 59123456PB, 59123456ZA, 59123456ZB

Indicate quantity of a single type of artifact received but not scanned. Create individual artifact folder/box and artifact number for each Artifact Type.

<input type="checkbox"/>	CD(s) containing:	<input type="checkbox"/>
	computer program listing	
	Doc Code: Computer	Artifact Type Code: P
	pages of specification	
	and/or sequence listing	<input type="checkbox"/>
	and/or table	
	Doc Code: Artifact	Artifact Type Code: S
	content unspecified or combined	<input type="checkbox"/>
	Doc Code: Artifact	Artifact Type Code: U

<input type="checkbox"/>	Stapled Set(s) Color Documents or B/W Photographs
	Doc Code: Artifact    Artifact Type Code: C

<input type="checkbox"/>	Microfilm(s)
	Doc Code: Artifact    Artifact Type Code: F

<input type="checkbox"/>	Video tape(s)
	Doc Code: Artifact    Artifact Type Code: V

<input type="checkbox"/>	Model(s)
	Doc Code: Artifact    Artifact Type Code: M

<input type="checkbox"/>	Bound Document(s)
	Doc Code: Artifact    Artifact Type Code: B

<input type="checkbox"/>	Confidential Information Disclosure Statement or Other Documents marked Proprietary, Trade Secrets, Subject to Protective Order, Material Submitted under MPEP 724.02, etc.
	Doc Code: Artifact    Artifact Type Code X

<input type="checkbox"/>	Other, description: _____
	Doc Code: Artifact    Artifact Type Code: Z